

Madison to the City of Hope Animal Resources Center and naturally colonized the mice with bacteria by handling and feeding a nonirradiated diet (catalogue no. 5001 Laboratory Rodent Diet; Purina Mills, Inc., Richmond, IN) for 1 month, then switching to an irradiated diet. The non-SPF colony was fed with nonirradiated Laboratory Rodent Diet with 6% fat (catalogue no. 5001). Breeders in SPF and non-SPF colonies were fed, respectively, with irradiated and nonirradiated Mouse Diet 9F containing 9% fat (catalogue no. 5020) to maintain health. The original non-SPF colony and the SPF colony were kept in separate rooms and maintained in polycarbonate microisolator cages. The GF colony was fed with Autoclavable Rodent Diet with 6% fat (catalogue no. 5010). All mice had free access to food and water. The City of Hope Research Animal Care Committee approved the housing and care for our mouse colonies.

**Tumor Analysis.** Six non-SPF mice 5 months of age were found dead or appeared moribund and were thus euthanized for cause. Four of these mice had tumors. The remaining asymptomatic mice not warranting euthanasia were thus examined after 5 months of age to evaluate tumor prevalence. We visually examined the entire length of the small and large intestine of every animal sacrificed for any abnormal growth or tumor formation. In most cases, we excised tumors and made Swiss rolls on the remaining ileum and colon to avoid missing small lesions (24). All tissue samples were fixed in 10% formalin in phosphate buffer and then processed for sectioning. Most sections

were stained with H&E for histological analysis. Only those lesions that had dysplastic histology (as defined below) examined by our staff pathologists were scored as tumors. Goblet cells were stained with Alcian Blue and counterstained with Nuclear Fast Red.

The tumors were analyzed for the stages of cancer progression described by Riddell *et al.* (2). Because of the nature of the GPX-DKO intestinal epithelium, which always had focal inflammation or pathology in the presence of luminal microflora, we did not include hyperplastic epithelium, which only showed crypt distortion or enlarged and branched glands as seen in polyps, as tumors. We scored tumors with low-grade dysplasia and high-grade dysplasia as precancerous lesions; cancers included both invasive carcinomas and signet-ring cell malignancies. The criteria for low-grade dysplasia were hyperplasia with cytological abnormalities, primarily loss of nuclear polarity, marked stratification of nuclei, nuclear hyperchromatism, and cellular and nuclear pleomorphism. High-grade dysplasia was scored when dysplastic epithelium extended to the apical surface or involved a large area. High-grade dysplasia also included carcinoma *in situ*, which has neoplastic epithelium forming a complex cribriform pattern (back-to-back glands with no intervening stroma) yet without evidence of invasion into the muscularis mucosa. Invasive carcinoma was scored when the atypical glands were seen in the muscularis mucosa, serosal adipose tissue, or muscle layers.

Logistic regression was used to test the association of cancer prevalence

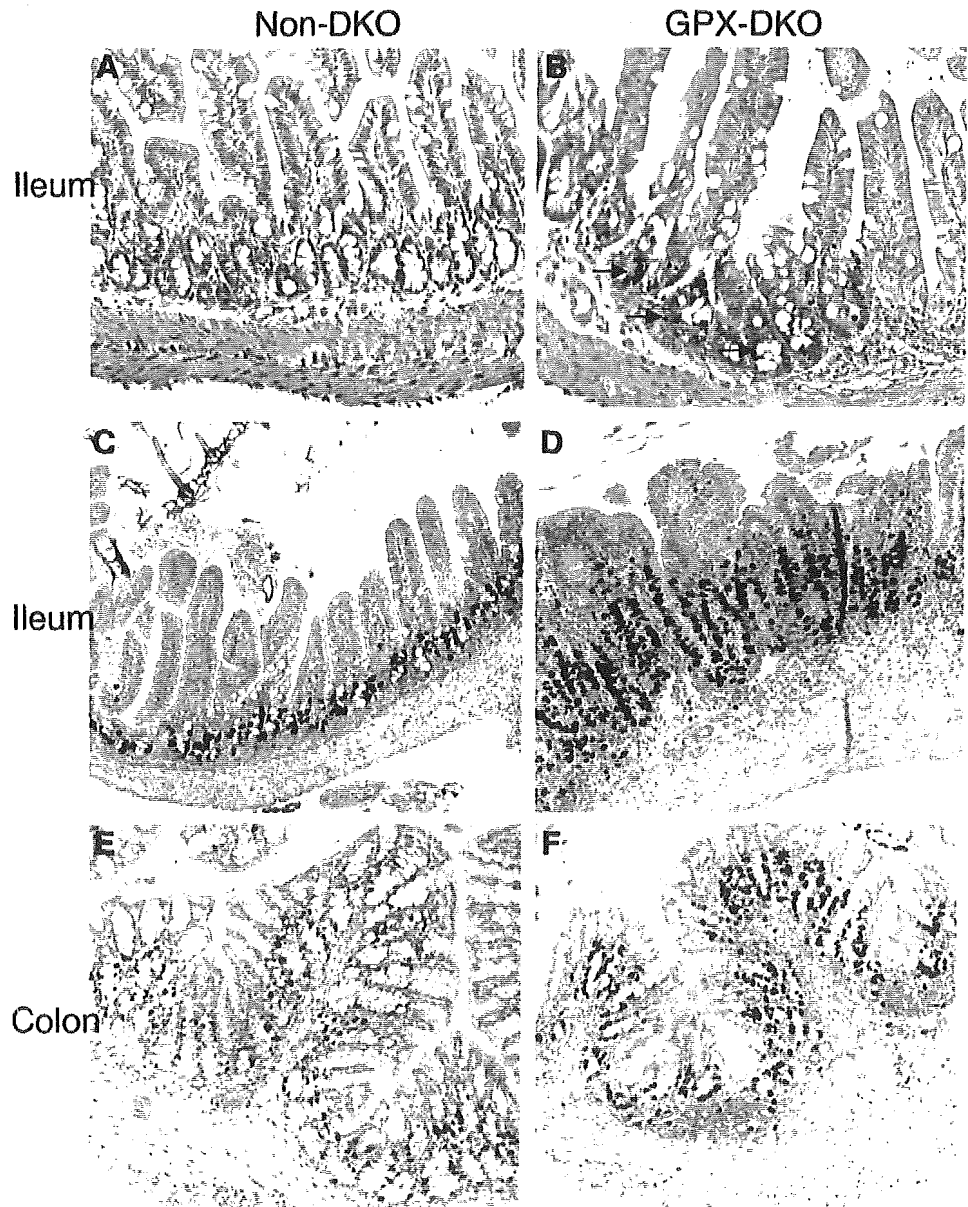


Fig. 1. Immunohistochemical staining of apoptotic cells in the ileum of 10-week-old germ-free mice and proliferating cells in the ileum and colon of 10-week-old specific pathogen-free mice. *A* and *B* demonstrate the apoptotic cells detected by terminal deoxynucleotidyl transferase assay, and the incorporated biotinylated deoxynucleotides were visualized with peroxidase staining. The tissues were counterstained with methyl green. *A* is an ileum of a GPX-DH mouse (*Gpx1*<sup>-/-</sup> *Gpx2*<sup>-/-</sup>) with no positive staining, and *B* is an ileum of a GPX-DKO mouse with dark brown positive staining (arrows). Both mice were euthanized on the day of arrival from the University of Wisconsin-Madison in germ-free isolators. *C-F* demonstrate mitotic cells in the ileum and colon of specific pathogen-free mice. Mice were injected with BrdUrd 2 h before euthanasia. BrdUrd was detected using an anti-BrdUrd antibody and visualized with streptavidin-peroxidase and 3,3'-diaminobenzidine, then cells were counterstained with hematoxylin. *C* and *E* are a GPX-DH and a 3/4-DKO mouse with (*Gpx1*<sup>-/-</sup> *Gpx2*<sup>-/-</sup>), and *D* and *F* are two GPX-DKO mice. The original magnification of *A* and *B* is 200, and *C-F* is 100. The apparently larger size of the GPX-DKO mouse ileum is due to underlying pathology.

with age at sacrifice, sex, parity, and colony conditions, each factor being adjusted for the others. Significant ( $P < 0.05$ ) likelihood-ratio tests with multiple degrees of freedom were followed by specific contrasts (Wald tests).

**Immunohistochemistry.** Mouse monoclonal anti- $\beta$ -catenin (1  $\mu$ g/ml) antibody (BD Transduction Labs) was used to determine cellular localization of  $\beta$ -catenin, which was detected with horseradish peroxidase and 3,3'-diaminobenzidine (Ultraspection Detection System; Lab Vision Co., Fremont, CA). Cell proliferation was detected with a BrdUrd immunohistochemistry kit (Oncogene Research Products, San Diego, CA). Mice were injected i.p. with 5-bromo-2'-deoxyuridine (BrdUrd, 120 mg/kg) and 5-fluoro-2'-deoxyuridine (12 mg/kg) dissolved in sterile Ringer's solution. Mice were euthanized 2 h after injection, and the small and large intestines were processed for routine paraffin embedding. Apoptotic cells were detected *in situ* by a TdT-FragEL DNA Fragmentation Detection kit (Oncogene) on the paraffin-embedded tissue sections. Rabbit polyclonal anti-myeloperoxidase antibody (7  $\mu$ g/ml; DakoCytomation, Carpinteria, CA) was used to detect polymorphonuclear neutrophils and monocytes (25). The proliferative index (stained cells/crypt) was determined by counting the number of stained cells in at least seven crypts of the most distorted region of the intestine for each mouse.

**RESULTS**

GPX-DKO mouse intestinal epithelium is highly susceptible to bacteria-induced pathology and inflammation. GF GPX-DKO mice have no pathology or symptoms except after shipping, which induces a temporary increase in crypt apoptosis and proliferation in the ileum (Fig. 1, A and B). When bacterial colonization occurs at birth, the ileal and colonic epithelium always exhibits focal pathology or inflammation throughout the life of the GPX-DKO mice (Fig. 2). The pathology and inflammation was scored in nontumorous areas based on a 17-point system, which includes inflammation as shown by lymphocyte or neutrophil infiltration (0–3 points), mucin depletion (0–2 points), reactive epithelium such as crypt distortion (0–3 points), number of intraepithelial lymphocytes (0–3 points), inflammatory foci (0–3 points), and apoptotic figures (0–3 points; Ref. 12). The pathology/

Table 1 Tumor incidence in mouse ileum and colon

| Age (months)                        | DKO                                  |                         |                      | Non-DKO <sup>a</sup> |           |         |
|-------------------------------------|--------------------------------------|-------------------------|----------------------|----------------------|-----------|---------|
|                                     | Male                                 | NB <sup>b</sup> -Female | Breeder <sup>b</sup> | Male                 | NB-Female | Breeder |
| Non-SPF colony <sup>a</sup>         |                                      |                         |                      |                      |           |         |
| 4.0–5.9                             | 8/20 <sup>c</sup> (40%) <sup>c</sup> | 1/8 (13%)               | — <sup>c</sup>       | 0/13                 | 0/7       | 0/1     |
| 6.0–8.9                             | 10/64 (16%)                          | 3/19 (16%)              | 3/9 (33%)            | 0/38                 | 0/16      | 0/1     |
| 9.0–13.0                            | 6/15 (40%)                           | 0/4 (0%)                | 5/9 (56%)            | 0/16                 | 0/4       | 0/2     |
| All ages                            | 24/99 (24%)                          | 4/31 (13%) <sup>c</sup> | 8/18 (44%)           | 0/67                 | 0/27      | 0/4     |
| SPF colony <sup>a</sup>             |                                      |                         |                      |                      |           |         |
| 4–5.9                               | 2/12 (17%)                           | 0/4                     | 0/2                  | 0/5                  | 0/1       | 0/1     |
| 6.0–8.9                             | 4/46 (9%)                            | 0/13                    | —                    | 0/20                 | 0/6       | —       |
| 9.0–13.0                            | 0/11 (0%)                            | —                       | —                    | 0/14                 | —         | —       |
| All ages                            | 6/69 (9%)                            | 0/17                    | 0/2                  | 0/39                 | 0/7       | 0/1     |
| SPF→non-SPF at weaning <sup>a</sup> |                                      |                         |                      |                      |           |         |
| 4–5.9                               | 0/1                                  | —                       | —                    | 0/2                  | —         | —       |
| 6.0–7.9                             | 4/13 (31%)                           | —                       | —                    | 0/8                  | —         | —       |
| All ages                            | 4/14 (27%)                           | —                       | —                    | 0/10                 | —         | —       |
| GF colony <sup>a</sup>              |                                      |                         |                      |                      |           |         |
| 4.0–5.9                             | 0/13                                 | 0/4                     | —                    | 0/6                  | —         | —       |
| 6.0–8.9                             | 0/2                                  | 0/3                     | 0/9                  | 0/1                  | 0/2       | —       |
| 9.0–12.0                            | 0/6                                  | —                       | 1/8 <sup>d</sup>     | 0/2                  | —         | 0/5     |
| All ages                            | 0/21                                 | 0/7                     | 1/17 (6%)            | 0/9                  | 0/2       | 0/5     |

<sup>a</sup> The conventionally reared specific pathogen-free (SPF) mice did not have detectable pathogens, and non-SPF mice harbored *Helicobacter* species, including *H. hepaticus*. Germ-free (GF) mice were derived from non-SPF mice and housed under GF conditions, and SPF mice were established from GF mice. The SPF→non-SPF colony contains mice transferred from SPF containment at 4 weeks of age to cages with soiled bedding from non-SPF mice. Non-DKO mice were littermates of the GPX-DKO mice with one wild-type *Gpx1* or *Gpx2* allele or double heterozygous KO.

<sup>b</sup> NB stands for non-breeder. Breeder consists of female mouse with one or more parity.

<sup>c</sup> The numerator is the number of mice with dysplasia and adenocarcinoma in the ileum or colon, and the denominator is the number of mice analyzed. Number in the parenthesis is the percentage of mice bearing tumors. Dash means no mice were analyzed in the category.

<sup>d</sup> A 9.1-month-old GF female breeder had an invasive ileal carcinoma.

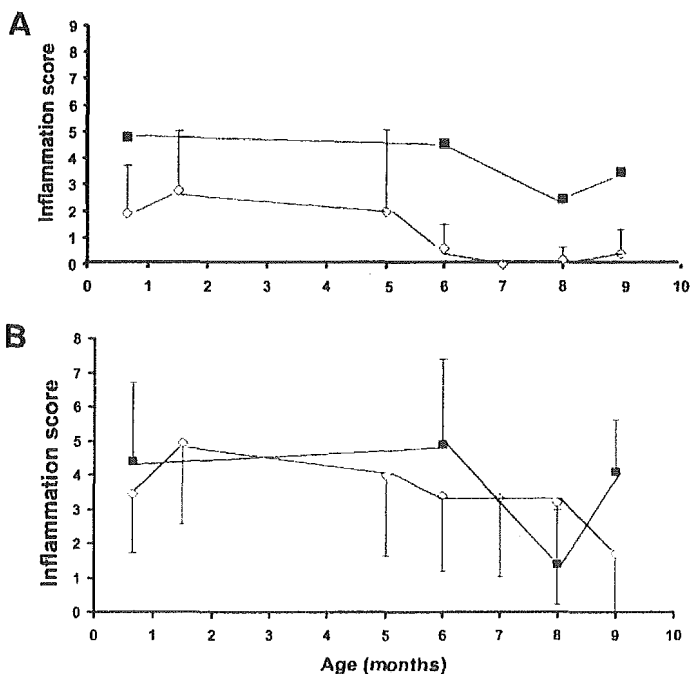


Fig. 2. Comparison of the mean inflammation/pathology scores (SD) between the non-specific-pathogen-free (non-SPF; ■) and the SPF (○) colonies in the ileum (A) and in the colon (B) by age. Only one-sided error bars are shown for clarity. Between 5 and 15 mice were analyzed at each time point. The ilea of the mice in the non-SPF colony had significantly higher inflammation/pathology scores than those of the SPF colony at matched ages ( $P < 0.04$  for each time point, *t* test). Colonic inflammation/pathology scores were similar for the non-SPF and SPF colonies.

inflammation scores in GPX-DKO ileal epithelium vary in degree based on exposure to microflora, with scores greatest in non-SPF SPF GF non-DKO mice. In colonic epithelium, the order of pathology scores was non-SPF SPF GF non-DKO (Fig. 2). SPF mouse ilea have significantly lower inflammation scores than non-SPF ilea when compared by age ( $P < 0.04$ , *t* test), whereas the colon scores remain the same (with *P*s ranging between 0.06 and 0.37, *t* test). We have previously reported that colonization with SPF microflora of adult GF GPX-DKO mice caused acute ileocolitis (26). Similarly, colonization with non-SPF microflora at weaning (4 weeks old) of the SPF GPX-DKO mice also caused acute ileocolitis, which resulted in one death in a group of 15 at the 53rd day after transfer. These transferred (SPF→non-SPF) GPX-DKO mice had similar inflammation scores as non-SPF GPX-DKO mice when analyzed 4–6 months later. On the basis of these observations, we conclude that non-SPF microflora provoked a more severe and persistent pathology than SPF microflora in the ilea of GPX-DKO mice.

Most of the pathology/inflammation scores are reflective of high numbers of focally appearing mitotic and apoptotic cells in the ileum and colon, with a small number of infiltrating neutrophils. We compared the extent of cell proliferation in the ileal and colonic crypts of SPF GPX-DKO and non-DKO littermates using a mitotic index (MI) scale 2 h after bromodeoxyuridine injection (Fig. 1 C, D, E, and F). At least seven crypts were counted in the most distorted regions. The ilea of GPX-DKO mice had 2.2-fold higher numbers of proliferating cells than non-DKO control mice. The ileal MI for GPX-DKO mice was 17.5 (mean SD,  $n = 5$ ) labeled cells/crypt and that for non-DKO (with one or one each wild-type *Gpx1* and *Gpx2* allele) 8.4 ( $n = 6$ ;  $P < 0.004$ , Wilcoxon test). Similarly, colonic crypts of GPX-DKO mice also had significantly higher numbers of proliferating cells than in non-DKO mice. The colonic MI for GPX-DKO was 11.2 ( $n = 4$ ) and for non-DKO 4.2 ( $n = 4$ ;  $P < 0.03$ , Wilcoxon

test). This higher MI in GPX-DKO mice may be necessary to avoid crypt atrophy caused by high levels of apoptosis. We found a lower number of ileal crypts (68 8/cross-section,  $n = 5$ ) in GPX-DKO mice compared with non-DKO mice (95 19/cross section,  $n = 5$ ,  $P = 0.03$ ) at 7–10 weeks of age. This suggests that the crypt loss due to apoptosis may not be fully compensated by a higher MI.

To determine tumor incidence, we euthanized mice primarily between 5 and 9 months of age in non-SPF, SPF, SPF→non-SPF, and GF colonies (Table 1). Because age variation at sacrifice could confound comparisons among the colonies, we adjusted for age variation by using a logistic regression test. We found age at sacrifice was not significantly associated with tumor prevalence ( $P = 0.3$ ). However, tumor prevalence varied significantly across colony conditions after adjustments for age and sex ( $P = 0.0001$ , 3 degrees of freedom,

logistic regression test; Table 1). The effect was primarily due to the difference between “the clean conditions” (the GF and SPF) as opposed to “the dirty conditions” (non-SPF and SPF→non-SPF conditions;  $P = 0.0003$ ). Comparisons within the clean and dirty conditions were not statistically significant ( $P = 0.15$  between GF and SPF, and  $P = 0.7$  between non-SPF and SPF→non-SPF). However, the data are consistent with the hypothesis that the risk of developing a tumor to GPX-DKO mice in SPF conditions was intermediate between that in GF and non-SPF conditions. The tumor rate among females varied significantly with parity adjusted for age and conditions, with non-breeder females having significantly fewer tumors ( $P = 0.02$ ). Male mice were not statistically distinguishable from either group of females ( $P = 0.07$ ). No tumors were found under any conditions in mice that had at least one wild-type *Gpx1* or *Gpx2* allele. These non-DKO

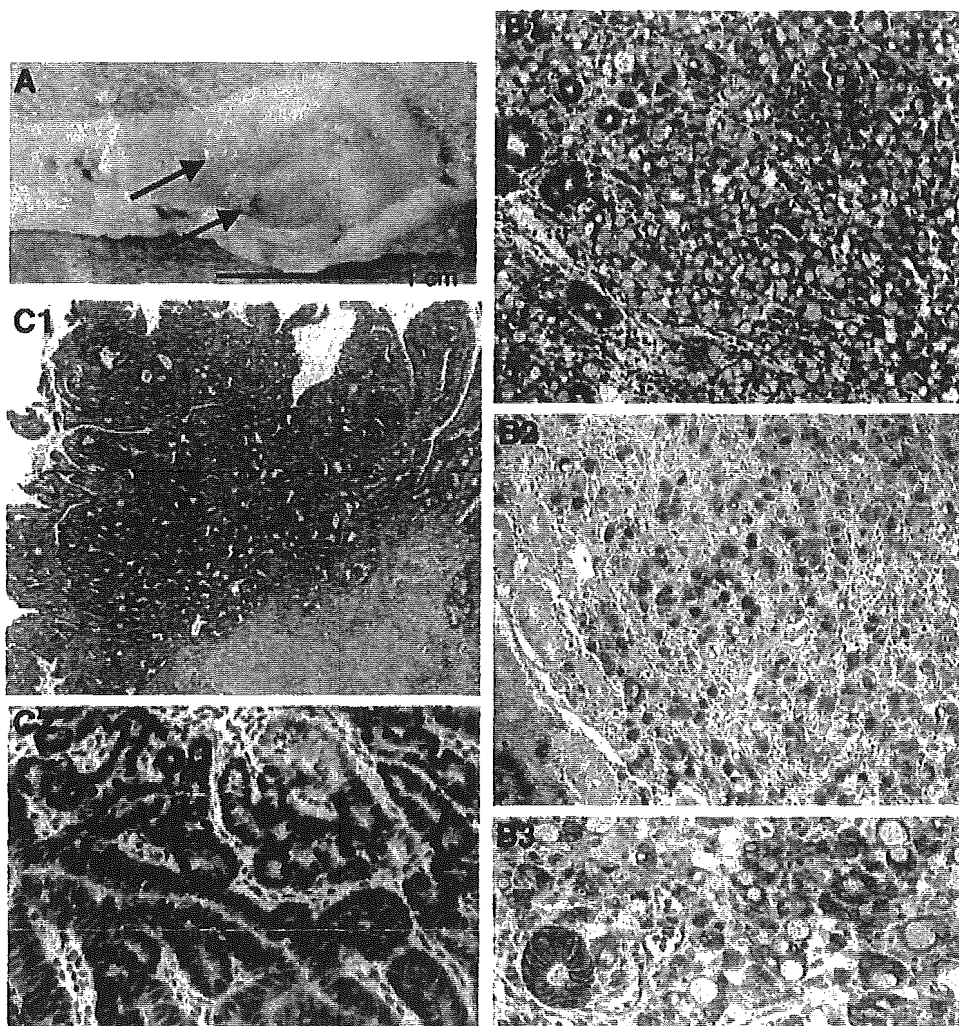


**Fig. 3.** Histopathology of tumors from GPX-DKO mice. **A** demonstrates a nonpolypoid tumor mass in the ileum with arrows pointing to the periphery of the 1-cm tumor. **B1** and **C1** are a signet-ring cell carcinoma (100) and an invasive adenocarcinoma (40) stained with H&E. The signet-ring cell carcinoma has abundant Alcian blue-stained mucin with a Nuclear Fast Red counterstain (**B2**). **B3** shows membranous  $\beta$ -catenin localization, and **C2** illustrates nuclear accumulation of  $\beta$ -catenin in this invasive cancer (both panels are originally amplified 200). **D** correlates the ileal epithelial inflammation/pathology scores with tumor incidence in male non-specific pathogen-free GPX-DKO mice. Ileal histology is shown for mice free of tumors (□) and with ileal tumors (■). Scoring criteria included lymphocytic or neutrophilic infiltration (0–3 points), mucin depletion (0–2 points), reactive epithelium such as crypt distortion (0–3 points), number of intraepithelial lymphocytes (0–3 points), inflammatory foci (0–3 points), and apoptotic figures (0–3 points). A significant difference was noted in scores for tumor-bearing (mean SD; 6.1 1.8,  $n = 16$ ) and nontumor bearing (4.1 3.0,  $n = 29$ ) mice ( $P = 0.04$ , Wilcoxon rank-sum test with continuity correction).

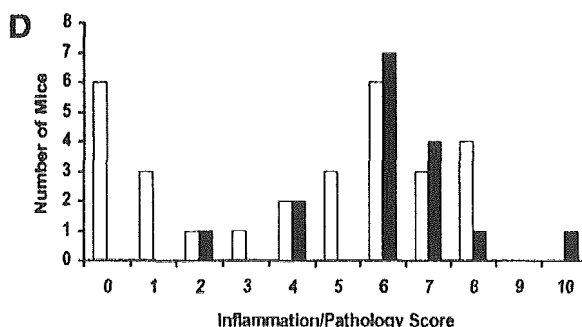


Table 2 Histological analysis of intestinal tumors in GPX-DKO mice

| Colony           | Age (months) | n <sup>a</sup> | LG dysplasia            | HG dysplasia             | Cancer <sup>b</sup>     |
|------------------|--------------|----------------|-------------------------|--------------------------|-------------------------|
| Non-SPF          | 5–12         | 36             | 10 (28%) <sup>c</sup>   | 16 (44%)                 | 10 (28%)                |
| SPF              | 2–8          | 6              | 4 (66%)                 | 2 (33%)                  | 0                       |
| SPF→non-SPF      | 7            | 4              | 0                       | 2 (50%)                  | 2 (50%)                 |
| GF               | 10           | 1              | 0                       | 0                        | 1 (100%)                |
| Total            | All ages     | 47             | 14 (30%)                | 20 (43%)                 | 13 (28%)                |
| Nuclear -catenin |              | 47             | 7/14 (50%) <sup>d</sup> | 19/20 <sup>e</sup> (95%) | 9/13 <sup>f</sup> (69%) |

<sup>a</sup> n, number of tumor-bearing mice in the colony; LG, low grade; HG, high grade; SPF, specific pathogen-free.

<sup>b</sup> Thirteen cancers include 10 invasive adenomas and 3 signet-ring cell carcinomas (SRCC). Three ileal SRCC were found in a 5-month-old and a 6-month-old non-SPF male mouse, as well as a 7-month-old male mouse transferred from SPF to non-SPF at weaning.

<sup>c</sup> The number in the parenthesis is the percentage of tumors exhibiting the specified histology in the colony.

<sup>d</sup> The number in the parenthesis is the percentage of tumors with nuclear -catenin accumulation within the characterized group.

<sup>e</sup> One HG-dysplastic tumor from a 10-month-old breeder non-SPF female did not have nuclear accumulation of -catenin.

<sup>f</sup> Three SRCC and an invasive tumor from a 7-month-old male mouse transferred from SPF to non-SPF at weaning did not have nuclear accumulation of -catenin.

mice were littermates of GPX-DKO mice and shared identical housing conditions. These observations exclude genetic background, non-intestinal environmental and dietary factors as etiologies for cancer susceptibility in this model.

All tumors were nonpolypoid masses 3 mm in diameter on inspection (Fig. 3A). Most mice had single tumors, except for a few mice that had 2 tumors each. Ten of 36 (28%) tumors analyzed in the non-SPF colony (from birth) were adenocarcinomas with 8 invasive carcinomas and two signet-ring cell carcinoma (SRCC; Table 2). Two of 4 tumors in the SPF→non-SPF colony were cancerous with 1 invasive and 1 SRCC. Most of the tumors were located in the distal ileum, except for 1 non-SPF mouse that had a tumor in the distal jejunum. Six mice had colonic tumors; this includes 1 SPF female, 1 SPF→non-SPF male, and 4 SPF male GPX-DKO mice.

Multiple gene mutations have been reported during colorectal carcinogenesis, and mutations in the *adenomatous polyposis coli* (*Apc*) gene occur often in both sporadic tumors and with colitis-associated cancers (27–32). The tumor suppressor activity of *Apc* sequesters the bifunctional -catenin for degradation. Cells with mutant *Apc* genes have detectable accumulations of cytoplasmic and nuclear -catenin (33–35). We stained for -catenin and used nuclear accumulation, only, as indirect evidence for *Apc* inactivation because it was difficult to distinguish cytoplasmic staining from background staining. We found that 7 of 14 (50%) low-grade dysplastic adenomas, 19 of 20 (95%) high-grade dysplastic adenomas, and 9 of 13 (69%) adenocarcinomas had nuclear accumulation of -catenin, including an invasive ileal adenocarcinoma in a GF breeder (Table 2 and Fig. 3). Two SRCCs from the non-SPF colony and 1 from the SPF→non-SPF colony did not show nuclear accumulation of -catenin (Fig. 3). Signet-ring morphology appeared to be caused by the large amounts of mucin (stained by Alcian Blue) pressing nuclei against the plasma membrane. The only invasive adenocarcinoma that did not have nuclear accumulation of -catenin was from the SPF→non-SPF colony.

The higher ileal tumor rates in non-SPF mice than SPF and GF mice correlated with higher pathology scores. Among the male non-SPF GPX-DKO mice, we also found that tumor-bearing mice had significantly higher ileal pathology scores than those that were tumor free (Fig. 3). Also, similar ileal scores were found between male (6.0 ± 2.4, n = 29) and female (6.6 ± 2.6, n = 12) GPX-DKO mice regardless of breeding status. However, although similar scores were found in the ileum and colon in the SPF colony, colon tumors were most prevalent.

## DISCUSSION

In this article, we provide the first direct evidence that GPX prevents ileocolitis and intestinal cancer. Elevation of reactive metabolites of oxygen and nitrogen during the inflammatory response are believed to cause some of the intestinal and colonic injury and dysfunction observed in IBD (17). However, most studies have focused on the damaging effect of superoxide and nitric oxide; few studies have examined the effect of hydroperoxides. Some indirect evidence suggests a protective role for *Gpx1* and *Gpx2* genes against oxidative stress. These data include induction of *Gpx1* gene expression in gastric mucosa by *H. pylori* infection (36) and induction of *Gpx2* gene expression in intestinal mucosa by commensal bacteria or by -irradiation (26, 37). However, elevated GPX gene expression has also been associated with tumorigenesis, presumably because of its antiapoptotic activity (38). Elevated *Gpx2* gene expression is observed in squamous cell carcinomas, Barrett's mucosa, and colorectal adenomas compared with normal tissues (39–41), and overexpression of the *Gpx1* gene increases skin cancer risk (42). Therefore, it has been a quandary whether increased GPX activity is anti-inflammatory or procarcinogenic. Our results suggest that GPX can prevent tumorigenesis in intestinal epithelium by its antioxidant activity.

The tumor incidence that we observed in the ilea of GPX-DKO mice is correlated with pathology/inflammation scores, with the highest cancer rate occurring in the non-SPF colony or SPF mice made non-SPF at weaning. However, the colon shows no correlation between the tumor incidence and pathology/inflammation scores. Both non-SPF and SPF colonies have similar pathology/inflammation scores in the colon, but SPF mice have more colonic tumors than non-SPF mice. Also, female non-SPF GPX-DKO mice had similar inflammation scores regardless of their breeding status. These results suggest that inflammatory changes are necessary but not sufficient for tumorigenesis.

Although male mice did not have a significantly higher tumor incidence than female mice, breeder females appeared to have a higher tumor incidence than nulliparous females. It has been noted that *H. hepaticus* causes more severe hepatic lesions in male mice, and *H. pylori* causes more severe intestinal-type gastritis and gastric cancer in men and male mice (19, 43, 44). Apparently, those microflora harbored in the non-SPF colony, from which most tumor-bearing mice were derived, did not have as strong an effect on ileal and colonic cancer incidence as *H. pylori* has on gastric cancer. In humans, parity is not recognized as a risk factor for colon cancer. However, it is unclear whether the pregnancy-associated risk in women with IBD can be obscured by decreased numbers of pregnancies due either to reduced fertility or choice and by more preterm births or smaller birth weights (45–47). Although we have found that multiparous female GPX-DKO mice had a significantly higher tumor incidence than nulliparous females because breeder females were on a diet with slightly higher fat content to promote their own and the litters' health and high-fat diet has been implicated in higher colorectal cancer risk (48), we cannot exclude the possibility that the different cancer rate is skewed by different diets. During normal pregnancy and preeclampsia, there is increased lipid peroxidation in multiple organs, which can increase oxidative DNA damage and gene mutations (49–52). Additional analysis will be needed to better evaluate whether parity increases cancer rate in GPX-DKO mice fed with the same 9% fat diet.

There are multiple sources for bacteria-induced oxidative stress. A few strains of commensal bacteria in *Enterococcus spp.* can generate reactive oxygen species in the lumen and cause inflammation-associated cancer in IL-10 KO mice (53–55). Epithelial cells also respond to bacterial colonization by modulating inflammatory responses (7, 9,

56). Colonization with *H. hepaticus* in A/JCr mice induces oxidative DNA damage in the liver and the expression of a subset of immune-related genes, including  $\gamma$ -IFN in cecal epithelium (57–59). *H. pylori* induces H<sub>2</sub>O<sub>2</sub> production and cyclooxygenase-2 expression in gastric epithelial cells (60). Although our results are consistent with the notion that *H. hepaticus* is pathogenic in GPX-DKO mice, additional studies are needed to fulfill Koch's postulates and to elucidate the molecular mechanism for bacteria-induced ileocolitis.

The tumor pathology in these mice is unique. Although most of tumors were adenomas, among 13 adenocarcinomas, there were 3 SRCCs. In humans, the occurrence of SRCC in the small intestine or colon is a rare but distinctive event, typically found in younger patients; it carries an adverse prognosis (61, 62). Few murine intestinal cancer models demonstrate signet-ring histology. Among the exceptions are the azoxymethane-induced colorectal cancer model in rats, duodenal polyps of *Smad4*-heterozygous mice, and intestinal tumors in *Smad4/Apc*-double heterozygous mice (16, 63–65). All 3 SRCCs in our GPX-DKO mice still had membranous  $\beta$ -catenin localization, suggesting that the *Wnt* pathway remains intact. This is consistent with the hypothesis that a set of genes other than those in the *Apc*- $\beta$ -catenin pathway may be mutated in SRCC (62, 64). This result also suggests that mutations in multiple pathways may occur during tumorigenesis in GPX-DKO mouse intestines.

Mutations in the *Apc* gene are a common early event in sporadic colon cancer. Whether *Apc* gene mutations occur as frequently in colitis-associated cancer is less certain (18). Opposing results have been found in mouse IBD models; IL-2/ $\beta$ -microglobulin-deficient mice have mutated *Apc* genes in all adenocarcinomas determined by DNA sequence analysis (32), but IL-10 deficient mice do not have *Apc* mutations in all tumors analyzed by immunohistochemistry of APC protein (66). Our results, showing most adenomas and non-SRCC adenocarcinomas have nuclear accumulation of  $\beta$ -catenin, support the notion that mutations in genes in the *Wnt* pathway occur in our inflammation-associated mouse model.

In summary, we have described a new mouse ileocolitis-associated cancer model. This is the first mouse ileal and colonic cancer model produced by a deficiency in antioxidant enzyme levels. Inflammation and cancer occurring in our GPX-DKO mice provide direct evidence, suggesting that intracellular hydroperoxides, which are reduced by GPX-1 and GPX-2, play an important role in cancer initiation, promotion, or progression. However, whether this goes beyond suppression of inflammation is not clear. Although some commensal microflora may be harmless or even beneficial to the host by preventing inflammation in intestinal mucosa (67, 68), certain luminal bacteria may drastically increase cancer incidence.

## ACKNOWLEDGMENTS

We thank Terri Armenta of the City of Hope Animal Resources Center, JoAnne Croft at the Gnotobiotic Lab, University of Wisconsin-Madison, and Kathryn A. Eaton, DVM, Ph.D., at Ohio State University-Columbus for providing housing and management of animals. We also thank Sophia Loera and Tina Montgomery of the Anatomical Pathology Core laboratory of the City of Hope Comprehensive Cancer Center for processing animal tissues.

## REFERENCES

- Guarner, F., and Malagelada, J. R. Gut flora in health and disease. *Lancet*, 361: 512–519, 2003.
- Riddell, R. H., Goldman, H., Ransohoff, D. F., Appelman, H. D., Fenoglio, C. M., Haggitt, R. C., Ahren, C., Correa, P., Hamilton, S. R., Morson, B. C., et al. Dysplasia in inflammatory bowel disease: standardized classification with provisional clinical applications. *Hum. Pathol.*, 14: 931–968, 1983.
- Schultz, M., Tonkonogy, S. L., Sellon, R. K., Veltkamp, C., Godfrey, V. L., Kwon, J., Grenther, W. B., Balish, E., Horak, I., and Sartor, R. B. IL-2-deficient mice raised under germ-free conditions develop delayed mild focal intestinal inflammation. *Am. J. Physiol.*, 276: G1461–G1472, 1999.
- Sellon, R. K., Tonkonogy, S., Schultz, M., Dieleman, L. A., Grenther, W., Balish, E., Rennick, D. M., and Sartor, R. B. Resident enteric bacteria are necessary for development of spontaneous colitis and immune system activation in interleukin-10-deficient mice. *Infect. Immun.*, 66: 5224–5231, 1998.
- Kado, S., Uchida, K., Funabashi, H., Iwata, S., Nagata, Y., Ando, M., Onoue, M., Matsuoka, Y., Ohwaki, M., and Morotomi, M. Intestinal microflora are necessary for development of spontaneous adenocarcinoma of the large intestine in T-cell receptor chain and p53 double-knockout mice. *Cancer Res.*, 61: 2395–2398, 2001.
- Engle, S. J., Ormsby, I., Pawlowski, S., Boivin, G. P., Croft, M. E., Balish, E., and Doetschman, T. Elimination of colon cancer in germ-free transforming growth factor 1-deficient mice. *Cancer Res.*, 62: 6362–6366, 2002.
- Svanborg, C., Godaly, G., and Hedlund, M. Cytokine responses during mucosal infections: role in disease pathogenesis and host defence. *Curr. Opin. Microbiol.*, 2: 99–105, 1999.
- Ogawa, H., Fukushima, K., Sasaki, I., and Matsuno, S. Identification of genes involved in mucosal defense and inflammation associated with normal enteric bacteria. *Am. J. Physiol. Gastrointest. Liver Physiol.*, 279: G492–G499, 2000.
- Neish, A. S., Gewirtz, A. T., Zeng, H., Young, A. N., Hobert, M. E., Karmali, V., Rao, A. S., and Madara, J. L. Prokaryotic regulation of epithelial responses by inhibition of I  $\beta$ -ubiquitination. *Science (Wash. DC)*, 289: 1560–1563, 2000.
- Kryukov, G. V., Castellano, S., Novoselov, S. V., Lobanov, A. V., Zehntab, O., Guigo, R., and Gladyshev, V. N. Characterization of mammalian selenoproteomes. *Science (Wash. DC)*, 300: 1439–1443, 2003.
- Esworthy, R. S., Swiderek, K. M., Ho, Y. S., and Chu, F. F. Selenium-dependent glutathione peroxidase-G1 is a major glutathione peroxidase activity in the mucosal epithelium of rodent intestine. *Biochim. Biophys. Acta*, 1381: 213–226, 1998.
- Esworthy, R. S., Aranda, R., Martin, M. G., Doroshov, J. H., Binder, S. W., and Chu, F. F. Mice with combined disruption of *Gpx1* and *Gpx2* genes have colitis. *Am. J. Physiol. Gastrointest. Liver Physiol.*, 281: G848–G855, 2001.
- Panwala, C. M., Jones, J. C., and Viney, J. L. A novel model of inflammatory bowel disease: mice deficient for the multiple drug resistance gene, *mdr1a*, spontaneously develop colitis. *J. Immunol.*, 161: 5733–5744, 1998.
- Yamada, T., Mori, Y., Hayashi, R., Takada, M., Ino, Y., Naishiro, Y., Kondo, T., and Hirohashi, S. Suppression of intestinal polyposis in *Mdr1*-deficient *ApcMin* mice. *Cancer Res.*, 63: 895–901, 2003.
- Bhan, A. K., Mizoguchi, E., Smith, R. N., and Mizoguchi, A. Colitis in transgenic and knockout animals as models of human inflammatory bowel disease. *Immunol. Rev.*, 169: 195–207, 1999.
- Boivin, G. P., Washington, K., Yang, K., Ward, J. M., Pretlow, T. P., Russell, R., Besselsen, D. G., Godfrey, V. L., Doetschman, T., Dove, W. F., Pitot, H. C., Halberg, R. B., Itzkowitz, S. H., Groden, J., and Coffey, R. J. Pathology of mouse models of intestinal cancer: consensus report and recommendations. *Gastroenterology*, 124: 762–777, 2003.
- Pavlick, K. P., Laroux, F. S., Fuseler, J., Wolf, R. E., Gray, L., Hoffman, J., and Grisham, M. B. Role of reactive metabolites of oxygen and nitrogen in inflammatory bowel disease (1, 2). *Free Radic. Biol. Med.*, 33: 311–322, 2002.
- Seril, D. N., Liao, J., Yang, G. Y., and Yang, C. S. Oxidative stress and ulcerative colitis-associated carcinogenesis: studies in humans and animal models. *Carcinogenesis (Lond.)*, 24: 353–362, 2003.
- Solnick, J. V., and Schauer, D. B. Emergence of diverse *Helicobacter* species in the pathogenesis of gastric and enterohepatic diseases. *Clin. Microbiol. Rev.*, 14: 59–97, 2001.
- Ward, J. M., Anver, M. R., Haines, D. C., Melhorn, J. M., Gorelick, P., Yan, L., and Fox, J. G. Inflammatory large bowel disease in immunodeficient mice naturally infected with *Helicobacter hepaticus*. *Lab. Anim. Sci.*, 46: 15–20, 1996.
- Burich, A., Hershberg, R., Waggle, K., Zeng, W., Brabb, T., Westrich, G., Viney, J. L., and Maggio-Price, L. *Helicobacter*-induced inflammatory bowel disease in IL-10- and T cell-deficient mice. *Am. J. Physiol. Gastrointest. Liver Physiol.*, 281: G764–G778, 2001.
- Erdman, S. E., Poutahidis, T., Tomczak, M., Rogers, A. B., Cormier, K., Plank, B., Horwitz, B. H., and Fox, J. G. CD4<sup>+</sup>CD25<sup>+</sup> regulatory T lymphocytes inhibit microbially induced colon cancer in Rag2-deficient mice. *Am. J. Pathol.*, 162: 691–702, 2003.
- Maggio-Price, L., Shows, D., Waggle, K., Burich, A., Zeng, W., Escobar, S., Morrissey, P., and Viney, J. L. *Helicobacter bilis* infection accelerates and *H. hepaticus* infection delays the development of colitis in multiple drug resistance-deficient (*mdr1a*<sup>-/-</sup>) mice. *Am. J. Pathol.*, 160: 739–751, 2002.
- Moolenbeek, C., and Ruitenberg, E. J. The "Swiss roll": a simple technique for histological studies of the rodent intestine. *Lab. Anim.*, 15: 57–59, 1981.
- Baldus, S., Eisele, J. P., Mani, A., Castro, L., Figueroa, M., Chumley, P., Ma, W., Tousson, A., White, C. R., Bullard, D. C., Brennan, M. L., Lusis, A. J., Moore, K. P., and Freeman, B. A. Endothelial transcytosis of myeloperoxidase confers specificity to vascular ECM proteins as targets of tyrosine nitration. *J. Clin. Investig.*, 108: 1759–1770, 2001.
- Esworthy, R. S., Binder, S. W., Doroshov, J. H., and Chu, F. F. Microflora trigger colitis in mice deficient in selenium-dependent glutathione peroxidase and induce *Gpx2* gene expression. *Biol. Chem.*, 384: 597–607, 2003.
- Kinzler, K. W., and Vogelstein, B. Lessons from hereditary colorectal cancer. *Cell*, 87: 159–170, 1996.
- Haigis, K. M., Caya, J. G., Reichelderfer, M., and Dove, W. F. Intestinal adenomas can develop with a stable karyotype and stable microsatellites. *Proc. Natl. Acad. Sci. USA*, 99: 8927–8931, 2002.
- Potter, J. D. Colorectal cancer: molecules and populations. *J. Natl. Cancer Inst.* (Bethesda), 91: 916–932, 1999.

30. Aust, D. E., Terdiman, J. P., Willenbacher, R. F., Chang, C. G., Molinaro-Clark, A., Baretton, G. B., Loehrs, U., and Waldman, F. M. The APC/  $\beta$ -catenin pathway in ulcerative colitis-related colorectal carcinomas: a mutational analysis. *Cancer (Phila.)*, *94*: 1421–1427, 2002.
31. Odze, R. D., Brien, T., Brown, C. A., Hartman, C. J., Wellman, A., and Fogt, F. Molecular alterations in chronic ulcerative colitis-associated and sporadic hyperplastic polyps: a comparative analysis. *Am. J. Gastroenterol.*, *97*: 1235–1242, 2002.
32. Sohn, K. J., Shah, S. A., Reid, S., Choi, M., Carrier, J., Comiskey, M., Terhorst, C., and Kim, Y. I. Molecular genetics of ulcerative colitis-associated colon cancer in the interleukin 2- and  $\beta$ -microglobulin-deficient mouse. *Cancer Res.*, *61*: 6912–6917, 2001.
33. Inomata, M., Ochiai, A., Akimoto, S., Kitano, S., and Hirohashi, S. Alteration of  $\beta$ -catenin expression in colonic epithelial cells of familial adenomatous polyposis patients. *Cancer Res.*, *56*: 2213–2217, 1996.
34. Morin, P. J., Sparks, A. B., Korinek, V., Barker, N., Clevers, H., Vogelstein, B., and Kinzler, K. W. Activation of  $\beta$ -catenin-Tcf signaling in colon cancer by mutations in  $\beta$ -catenin or APC. *Science (Wash. DC)*, *275*: 1787–1790, 1997.
35. Liu, C., Li, Y., Semenov, M., Han, C., Baeg, G. H., Tan, Y., Zhang, Z., Lin, X., and He, X. Control of  $\beta$ -catenin phosphorylation/degradation by a dual-kinase mechanism. *Cell*, *108*: 837–847, 2002.
36. Maeda, S., Otsuka, M., Hirata, Y., Mitsuno, Y., Yoshida, H., Shiratori, Y., Masuho, Y., Muramatsu, M., Seki, N., and Omata, M. cDNA microarray analysis of *Helicobacter pylori*-mediated alteration of gene expression in gastric cancer cells. *Biochem. Biophys. Res. Commun.*, *284*: 443–449, 2001.
37. Esworthy, R. S., Mann, J. R., Sam, M., and Chu, F. F. Low glutathione peroxidase activity in Gpx1 knockout mice protects jejunal crypts from  $\gamma$ -irradiation damage. *Am. J. Physiol. Gastrointest. Liver Physiol.*, *279*: G426–G436, 2000.
38. Hockenbery, D. M., Oltvai, Z. N., Yin, X. M., Millman, C. L., and Korsmeyer, S. J. Bcl-2 functions in an antioxidant pathway to prevent apoptosis. *Cell*, *75*: 241–251, 1993.
39. Serewko, M. M., Popa, C., Dahler, A. L., Smith, L., Strutton, G. M., Coman, W., Dicker, A. J., and Saunders, N. A. Alterations in gene expression and activity during squamous cell carcinoma development. *Cancer Res.*, *62*: 3759–3765, 2002.
40. Mork, H., Scheurle, M., Al-Taie, O., Zierer, A., Kraus, M., Schotker, K., Jakob, F., and Kohrle, J. Glutathione peroxidase isoforms as part of the local antioxidative defense system in normal and Barrett's esophagus. *Int. J. Cancer*, *105*: 300–304, 2003.
41. Mork, H., al-Taie, O. H., Bahr, K., Zierer, A., Beck, C., Scheurle, M., Jakob, F., and Kohrle, J. Inverse mRNA expression of the selenocysteine-containing proteins GPx and SeP in colorectal adenomas compared with adjacent normal mucosa. *Nutr. Cancer*, *37*: 108–116, 2000.
42. Lu, Y. P., Lou, Y. R., Yen, P., Newmark, H. L., Mirochnitchenko, O. I., Inouye, M., and Huang, M. T. Enhanced skin carcinogenesis in transgenic mice with high expression of glutathione peroxidase or both glutathione peroxidase and superoxide dismutase. *Cancer Res.*, *57*: 1468–1474, 1997.
43. Fox, J. G., Rogers, A. B., Ihrig, M., Taylor, N. S., Whary, M. T., Dockray, G., Varro, A., and Wang, T. C. *Helicobacter pylori*-associated gastric cancer in INS-GAS mice is gender specific. *Cancer Res.*, *63*: 942–950, 2003.
44. Fox, J. G., Wang, T. C., Rogers, A. B., Poutahidis, T., Ge, Z., Taylor, N., Dangler, C. A., Israel, D. A., Krishna, U., Gaus, K., and Peek, R. M. J. Host and microbial constituents influence *Helicobacter pylori*-induced cancer in a murine model of hypergastrinemia. *Gastroenterology*, *124*: 1879–1890, 2003.
45. Katz, J. A., and Pore, G. Inflammatory bowel disease and pregnancy. *Inflamm. Bowel Dis.*, *7*: 146–157, 2001.
46. Moser, M. A., Okun, N. B., Mayes, D. C., and Bailey, R. J. Crohn's disease, pregnancy, and birth weight. *Am. J. Gastroenterol.*, *95*: 1021–1026, 2000.
47. Dominitz, J. A., Young, J. C., and Boyko, E. J. Outcomes of infants born to mothers with inflammatory bowel disease: a population-based cohort study. *Am. J. Gastroenterol.*, *97*: 641–648, 2002.
48. Kuwada, S. K. Colorectal cancer 2000. Education and screening are essential if outcomes are to improve. *Postgrad. Med.*, *107*: 96–107, 2000.
49. Little, R. E., and Gladen, B. C. Levels of lipid peroxides in uncomplicated pregnancy: a review of the literature. *Reprod. Toxicol.*, *13*: 347–352, 1999.
50. Sainz, R. M., Reiter, R. J., Mayo, J. C., Cabrera, J., Tan, D. X., Qi, W., and Garcia, J. J. Changes in lipid peroxidation during pregnancy and after delivery in rats: effect of pinealectomy. *J. Reprod. Fertil.*, *119*: 143–149, 2000.
51. Sacks, G. P., Studena, K., Sargent, K., and Redman, C. W. Normal pregnancy and preeclampsia both produce inflammatory changes in peripheral blood leukocytes akin to those of sepsis. *Am. J. Obstet. Gynecol.*, *179*: 80–86, 1998.
52. Sacks, G., Sargent, I., and Redman, C. Innate immunity in pregnancy. *Immunol. Today*, *21*: 200–201, 2000.
53. Mundy, L. M., Sahn, D. F., and Gilmore, M. Relationships between enterococcal virulence and antimicrobial resistance. *Clin. Microbiol. Rev.*, *13*: 513–522, 2000.
54. Huycke, M. M., Abrams, V., and Moore, D. R. *Enterococcus faecalis* produces extracellular superoxide and hydrogen peroxide that damages colonic epithelial cell DNA. *Carcinogenesis (Lond.)*, *23*: 529–536, 2002.
55. Balish, E., and Warner, T. *Enterococcus faecalis* induces inflammatory bowel disease in interleukin-10 knockout mice. *Am. J. Pathol.*, *160*: 2253–2257, 2002.
56. Kriegelstein, C. F., Cerwinka, W. H., Laroux, F. S., Salter, J. W., Russell, J. M., Schuermann, G., Grisham, M. B., Ross, C. R., and Granger, D. N. Regulation of murine intestinal inflammation by reactive metabolites of oxygen and nitrogen: divergent roles of superoxide and nitric oxide. *J. Exp. Med.*, *194*: 1207–1218, 2001.
57. Sipowicz, M. A., Chomarat, P., Diwan, B. A., Anver, M. A., Awasthi, Y. C., Ward, J. M., Rice, J. M., Kasprzak, K. S., Wild, C. P., and Anderson, L. M. Increased oxidative DNA damage and hepatocyte overexpression of specific cytochrome P450 isoforms in hepatitis of mice infected with *Helicobacter hepaticus*. *Am. J. Pathol.*, *151*: 933–941, 1997.
58. Singh, R., Leuratti, C., Josyula, S., Sipowicz, M. A., Diwan, B. A., Kasprzak, K. S., Schut, H. A., Marnett, L. J., Anderson, L. M., and Shuker, D. E. Lobe-specific increases in malondialdehyde DNA adduct formation in the livers of mice following infection with *Helicobacter hepaticus*. *Carcinogenesis (Lond.)*, *22*: 1281–1287, 2001.
59. Myles, M. H., Livingston, R. S., Livingston, B. A., Criley, J. M., and Franklin, C. L. Analysis of gene expression in ceca of *Helicobacter hepaticus*-infected A/JCr mice before and after development of typhlitis. *Infect. Immun.*, *71*: 3885–3893, 2003.
60. Kim, H., Seo, J. Y., and Kim, K. H. Effect of mannitol on *Helicobacter pylori*-induced cyclooxygenase-2 expression in gastric epithelial AGS cells. *Pharmacology (Basel)*, *66*: 182–189, 2002.
61. Kim, H. C., Kim, H. J., and Kim, J. C. Reduced E-cadherin expression as a cause of distinctive signet-ring cell variant in colorectal carcinoma. *J. Korean Med. Sci.*, *17*: 23–28, 2002.
62. Ooi, B. S., Ho, Y. H., Eu, K. W., and Seow Choen, F. Primary colorectal signet-ring cell carcinoma in Singapore. *ANZ J. Surg.*, *71*: 703–706, 2001.
63. Shamsuddin, A. K., and Trump, B. F. Colon epithelium. II. *In vivo* studies of colon carcinogenesis. Light microscopic, histochemical, and ultrastructural studies of histogenesis of azoxymethane-induced colon carcinomas in Fischer 344 rats. *J. Natl. Cancer Inst. (Bethesda)*, *66*: 389–401, 1981.
64. Takaku, K., Miyoshi, H., Matsunaga, A., Oshima, M., Sasaki, N., and Taketo, M. M. Gastric and duodenal polyps in Smad4 (Dpc4) knockout mice. *Cancer Res.*, *59*: 6113–6117, 1999.
65. Takaku, K., Oshima, M., Miyoshi, H., Matsui, M., Seidín, M. F., and Taketo, M. M. Intestinal tumorigenesis in compound mutant mice of both *Dpc4* (*Smad4*) and *Apc* genes. *Cell*, *92*: 645–656, 1998.
66. Sturlan, S., Oberhuber, G., Beinhauer, B. G., Tichy, B., Kappel, S., Wang, J., and Rogy, M. A. Interleukin-10-deficient mice and inflammatory bowel disease associated cancer development. *Carcinogenesis (Lond.)*, *22*: 665–671, 2001.
67. Hooper, L. V., Wong, M. H., Thelin, A., Hansson, L., Falk, P. G., and Gordon, J. I. Molecular analysis of commensal host-microbial relationships in the intestine. *Science (Wash. DC)*, *291*: 881–884, 2001.
68. Yan, F., and Polk, D. B. Probiotic bacterium prevents cytokine-induced apoptosis in intestinal epithelial cells. *J. Biol. Chem.*, *277*: 50959–50965, 2002.

## Elimination of Colon Cancer in Germ-free Transforming Growth Factor Beta 1-deficient Mice<sup>1</sup>

Sandra J. Engle, Ilona Ormsby, Sharon Pawlowski, Gregory P. Boivin, Joanne Croft, Edward Balish, and Tom Doetschman<sup>2</sup>

Departments of Molecular Genetics, Biochemistry and Microbiology [S. J. E., I. O., S. P., T. D.] and Comparative Pathology [G. P. B.], University of Cincinnati College of Medicine, Cincinnati, Ohio 45267-0524; Aventis Pharmaceuticals, Bridgewater, New Jersey 08807 [S. J. E.]; Department of Surgery, University of Wisconsin Medical School, Madison, Wisconsin 53706-1087 [J. C., E. B.]; and Department of Microbiology and Immunology, Medical University of South Carolina, Charleston, South Carolina 29425 [E. B.]

### Abstract

Patients with ulcerative colitis are at risk for colon cancer and frequently have microsatellite instability, which, in turn, is usually associated with inactivation of transforming growth factor (TGF) signaling. TGF-1 deficiency in mice can lead to colon cancer that is preceded by precancerous lesions having submucosal inflammation and hyperplastic crypts. Germ-free TGF-1-deficient mice are free of inflammation, hyperplasia, and cancer, but when reintroduced into a *Helicobacter hepaticus*-containing specific pathogen-free room, these lesions reappear. Because adenoma/carcinoma but not inflammation/hyperplasia is dependent on the genetic backgrounds tested, colitis is required, but not sufficient, for carcinogenesis. This animal model should provide insight into the protective role of TGF-1 in early stages of ulcerative colitis-associated human colon cancer.

### Introduction

TGF-1<sup>3</sup> is at the apex of a signaling pathway that is one of the more commonly disrupted pathways in human colon cancer (1). Human colon tumor-derived cell lines are frequently resistant to the growth-inhibitory effects of TGF-1 (2), and this loss of sensitivity often results from *TGFBR2* inactivating mutations. *TGFBR2* mutations are found in 90% of MSI-positive tumors, and therefore account for 13% of all human colon tumors (3). MSI is often associated with UC-associated colon cancer (4). Consequently, it is probable that inactivation of TGF- signaling also correlates with UC-associated colon cancer. The tumor suppressor effect of TGF-1 in humans is thought to occur at a late stage of tumorigenesis because microsatellite unstable tumors usually have *TGFBR2* mutations only if the tumors are at the adenoma/carcinoma transition stage or later (5). These studies indicate that causal relationships may exist among UC, TGF-signaling, genetic instability, and colon adenocarcinoma, but the basis of these relationships is unclear. Because TGF-1-deficient mice on an immunodeficient background develop colon cancer that is associated with inflammation (6), they would be a useful model for determining the relationship among UC, TGF-, and colon cancer if it could be demonstrated that the inflammatory lesions are required for tumorigenesis. To make this determination we have eliminated inflammatory bowel lesions by making germ-free TGF-1-deficient mice. Here we show that in the absence of enteric flora there is no inflammation, hyperplasia, or neoplasia, and that recolonization of the mice with enteric flora can result in the reappearance of colon cancer.

### Materials and Methods

A breeding pair of *Tgfb1*<sup>-/-</sup> *Rag2*<sup>-/-</sup> mice was generously provided by Dr. Robert L. Coffman (DNX Transgenics, Princeton, NJ, presently, Dynavax Technologies, Emeryville, CA). Specific pathogen-free breeding colonies of (a) *Tgfb1*<sup>-/-</sup> *Rag2*<sup>-/-</sup> mice with a mixed genetic background of 85–94% 129S2/SvPas (formerly 129/SvPas) and the remainder CF1; and (b) *Tgfb1*<sup>-/-</sup> *Prkdc*<sup>scid/scid</sup> mice with a mixed genetic background of 85–94% C3H/HeJ, and the remainder CF1 and 129S2/SvPas were housed in a barrier facility operated by the University of Cincinnati Laboratory Animal Medicine Services. Germ-free *Tgfb1*<sup>-/-</sup> *Rag2*<sup>-/-</sup> mouse colonies were established at the University of Wisconsin Gnotobiotic Research Laboratory (Madison, WI) by caesarean derivation. The establishment, maintenance, and health surveys of the barrier-raised and germ-free mice were carried out as reported (7, 8). PCR for *Helicobacter hepaticus* was carried out by the Research Animal Diagnostic and Investigative Laboratory, Columbia, MO.

When germ-free *Tgfb1*<sup>-/-</sup> *Rag2*<sup>-/-</sup> mice were reintroduced into our barrier facility for recolonization with the resident enteric flora, they were placed in two separate specific pathogen-free rooms, SPF1 and SPF2. SPF1 is the room where the animals with colon cancer had originally been housed, and SPF2 is a similar breeding room in the same barrier facility. Maintenance and quality control for the two rooms is identical, the only known difference being that SPF2 was *Helicobacter sp.*-free.

Histological examination and scoring for lesion classification was done as described previously (6). All of the analyses were performed blinded to prevent bias. A one-tailed Student *t* test was used for statistical analysis. Genotyping the secretory group II phospholipase A<sub>2</sub> wild-type (*Pla2g2a*, C3H strain) and mutant (*Pla2g2a*<sup>Mom1</sup>, 129 strain) alleles were identified by the PCR genotyping technique described previously (9). DSS treatment was performed on eight each of *Tgfb1*<sup>-/-</sup> *Prkdc*<sup>scid/scid</sup> and *Tgfb1*<sup>-/-</sup> *Prkdc*<sup>scid/scid</sup> 6–8 week-old mice as described (10). The concentration and duration of treatment were chosen to induce a chronic inflammation similar to that seen in the original *Tgfb1*<sup>-/-</sup> *Rag2*<sup>-/-</sup> SPF1 colony without inducing acute symptoms.

### Results and Discussion

From the outset it is necessary to make a clear distinction between the autoimmune-like multifocal inflammatory phenotype of *Tgfb1*<sup>-/-</sup> mice and the inflammatory lesions found in the cecums and colons of *Tgfb1*<sup>-/-</sup> *Rag2*<sup>-/-</sup> mice. Immunocompetent *Tgfb1*<sup>-/-</sup> mice have inflammatory lesions in multiple organs, and their median age of death is 20 days (11). When made germ-free, these mice still die from the autoimmune-like disease (7). However, if *Tgfb1*<sup>-/-</sup> mice are genetically combined with lymphocyte-deficient mice, such as *Rag2* knockout (6) or *Prkdc*<sup>scid/scid</sup> (12) mice, they are rescued from the autoimmune phenotype, and they can live as long as 8 months. However, submucosal, primarily granulocytic inflammatory lesions with accompanying hyperplasia now occur in the cecum and colon of these mice. These lesions occur in nearly all of the immunodeficient mice regardless of the presence or absence of TGF-1. Consequently, the inflammatory lesions that are associated with cecum and colon in *Tgfb1*<sup>-/-</sup> *Rag2*<sup>-/-</sup> mice are unrelated to the autoimmune-like inflammatory lesions of immunocompetent *Tgfb1*<sup>-/-</sup> mice (6).

Received 7/24/02; accepted 9/24/02.

The costs of publication of this article were defrayed in part by the payment of page charges. This article must therefore be hereby marked advertisement in accordance with 18 U.S.C. Section 1734 solely to indicate this fact.

<sup>1</sup> Supported by NIH Grants HD26471, CA84291, ES05652, and ES06096 (to T. D.).

<sup>2</sup> To whom requests for reprints should be addressed, at University of Cincinnati, 3110 Medican Sciences Building, 231 Bethesda Avenue, Cincinnati, OH 45267-0524.

<sup>3</sup> The abbreviations used are: TGF, transforming growth factor; *TGFBR2*, transforming growth factor receptor type II; MSI, microsatellite instability; UC, ulcerative colitis; DSS, dextran sodium sulfate.

**Genetic Background Effects on Carcinogenesis in TGF-1-deficient Mice.** Immunodeficient  $Tgfb1^{-/-}$   $Prkdc^{scid/scid}$  and  $Tgfb1^{-/-}$   $Rag2^{-/-}$  mice were placed on predominantly C3H or 129 genetic backgrounds, respectively. In both cases the animals were devoid of the autoimmune-like inflammatory disease described above. However, in each colony immunodeficient  $Tgfb1^{-/-}$  and  $Tgfb1^{-/-}$  animals developed submucosal inflammatory foci of the large intestine, and hyperplastic crypts were associated with the inflammatory lesions for  $Tgfb1^{-/-}$  or  $Rag2^{-/-}$  mice (6) and for  $Tgfb1^{-/-}$  or  $Prkdc^{scid/scid}$  mice (Fig. 1). However, only in immunocompromised TGF-1-deficient animals on a predominantly 129 background ( $Tgfb1^{-/-}$   $Rag2^{-/-}$  mice) was progression to adenoma and adenocarcinoma observed (see Fig. 1 in Ref. 6). These results suggest that there may be modifier genes present in 129 strains that increase susceptibility for progression from hyperplasia to adenoma, and that inflammation is required but not sufficient for the development of cecum and colon cancer in immunocompromised TGF-1-deficient mice on a 129-strain genetic background.

**Genetic Background Affects Susceptibility to Mouse Colon Cancer.** One modifier locus that has been implicated in modifying tumor development in the  $Apc^{Min}$  mouse can be identified by the secretory group II phospholipase  $A_2$  gene allele  $Pla2g2a^{Mom1}$ . The  $Pla2g2a^{Mom1}$  allele is a spontaneously occurring mutation propagated in specific strains of mice that results in severely deficient enzyme activity. It is linked to increased tumor numbers in  $Apc^{Min}$  mice on the 129 background compared with  $Apc^{Min}$  mice with a wild-type  $Pla2g2a$  allele, such as C3H mice. However, it is not completely clear whether the  $Pla2g2a^{Mom1}$  allele is responsible for the increased susceptibility (9). Because TGF-1-deficient mice are maintained on a partially mixed genetic background to circumvent embryonic lethality, some of the predominantly C3H-background  $Tgfb1^{-/-}$

$Prkdc^{scid/scid}$  mice should be homozygous for the  $Pla2g2a^{Mom1}$  susceptibility locus. Four such mice ranging in age from 4–6 months were identified and analyzed. Two had no lesions, one had inflammation and hyperplasia, and one had an adenoma (Fig. 2). One  $Tgfb1^{-/-}$  wild-type  $Prkdc^{scid/scid}$  mouse with the  $Pla2g2a^{Mom1}$  locus also had inflammation and hyperplastic lesions but no adenomas (data not shown). Because all of the  $Tgfb1^{-/-}$   $Rag2^{-/-}$  animals with *H. hepaticus* and the  $Pla2g2a^{Mom1}$  locus develop adenomas and adenocarcinomas, another modifier locus (loci) must account for most of the susceptibility in that strain. Consequently,  $Pla2g2a^{Mom1}$  could represent a weak modifier locus conferring a minor degree of susceptibility to colitis-induced colon cancer, but it does not account for the full penetrance of the colon cancer phenotype in predominantly 129  $Tgfb1^{-/-}$   $Rag2^{-/-}$  mice, because nearly all of the  $Tgfb1^{-/-}$   $Rag2^{-/-}$  mice develop colon cancer (6). Hence, there is at least one other major colon cancer susceptibility locus in strain 129 mice.

**Colitis Is Required but Not Sufficient for Carcinogenesis in  $Tgfb1^{-/-}$   $Rag2^{-/-}$  Mice.** A previous study demonstrated that barrier-raised  $Tgfb1^{-/-}$   $Rag2^{-/-}$  mice develop colon cancer from 3 to 6 months of age, and that inflammatory foci were always associated with the tumorigenic lesions, whereas the  $Tgfb1^{-/-}$  and  $Rag2^{-/-}$  mice infrequently developed lesions beyond hyperplasia (6). Assuming that some complement of normal and/or pathogenic microbial flora resulted in an inflammatory response that, in turn, induced the tumorigenic lesions, we reasoned that making the mice germ-free would eliminate the inflammation and subsequent cancer. Barrier-raised  $Tgfb1^{-/-}$   $Rag2^{-/-}$  mice were crossed, and the pregnant females were sent to the Gnotobiotic Facility in Madison, WI, where a germ-free standing colony of  $Tgfb1^{-/-}$   $Rag2^{-/-}$  mice was established. Eighteen germ-free  $Tgfb1^{-/-}$   $Rag2^{-/-}$  mice, 7  $Tgfb1^{-/-}$   $Rag2^{-/-}$  mice, and 6  $Tgfb1^{-/-}$   $Rag2^{-/-}$  mice ranging from 3 to 6

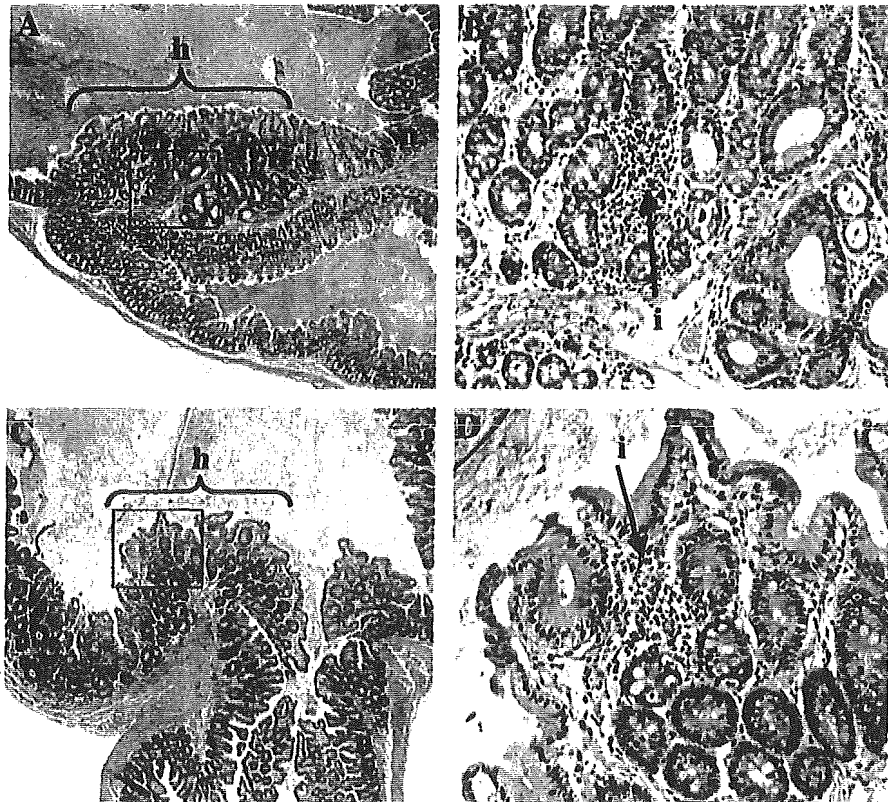


Fig. 1. Inflammation and hyperplasia in  $Tgfb1^{-/-}$  and  $Prkdc^{scid/scid}$  Mice. A, inflammation and hyperplasia in cecum of  $Tgfb1^{-/-}$   $Prkdc^{scid/scid}$  mice (10 magnification). B, 5-fold magnification of inset depicted in A. C, inflammation and hyperplasia in cecum of  $Tgfb1^{-/-}$   $Prkdc^{scid/scid}$  mice (10 magnification). D, 5-fold magnification of inset depicted in C. h, hyperplasia; i, inflammation.



*Pla2*<sup>+/+</sup> *Pla2*<sup>-/-</sup> *Scid Tgfb1*<sup>-/-</sup> mice (85-94% C3H)  
C3H 129

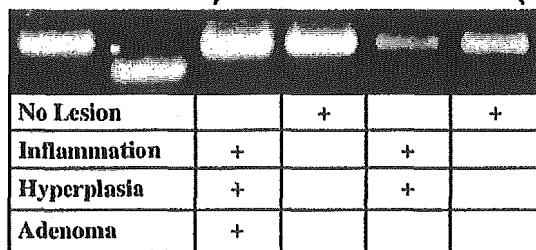


Fig. 2. *Pla2g2a*<sup>Momi</sup> is not a major colon tumor susceptibility locus in *Tgfb1*<sup>-/-</sup> *Rag2*<sup>-/-</sup> mice. The bottom PCR-generated band represents the wild-type *Pla2g2a* allele (*Pla2*<sup>+/+</sup>), which is present in C3H mice. The top band represents the mutant *Pla2g2a*<sup>Momi</sup> allele (*Pla2*<sup>-/-</sup>) that is present in 129 mice. *Tgfb1*<sup>-/-</sup> *Prkdc*<sup>scid/scid</sup> mice (predominantly C3H background) are represented in Lanes 3-6 and are all homozygous for the 129 strain *Pla2g2a*<sup>Momi</sup> susceptibility locus, yet only one of them (Lane 4) progressed beyond hyperplasia.

months of age were analyzed for hyperplastic, adenomatous, and neoplastic lesions, as well as for submucosal inflammatory foci. Fig. 3, A and B, compare histological sections of colon samples from the progenitor barrier-raised and germ-free colonies, respectively, demonstrating that the inflammatory bowel lesions had been eliminated by the germ-free conditions. None of the mice in this colony developed hyperplasia, adenoma, or adenocarcinoma, strongly suggesting that colitis is required for the development of colon cancer in TGF-1-deficient mice.

**Recolonization of Germ-free Mice with Enteric Flora.** To confirm that the presence of enteric microbial content can lead to tumorigenic cecum and colon lesions associated with inflammatory bowel foci, germ-free *Tgfb1*<sup>-/-</sup> *Rag2*<sup>-/-</sup> mice from the Wisconsin germ-free colony were reintroduced into two independent SPF rooms in the University of Cincinnati barrier facility. Within 1 year the incidence of colon cancer had reappeared in the SPF1 room where mice had been housed for the original colon cancer study (6). In contrast, no colon cancer has reappeared in 3 years in SPF2. Consistent with our previous results, colitis was always present in mice developing colon cancer in SPF1 (Fig. 3C) and was never present in SPF2 where mice were free of tumorigenic lesions (Fig. 3D). These results demonstrate that gut microbial content is integral to the development of colitis in *Rag2*<sup>-/-</sup> mice and to the development of colon cancer in *Tgfb1*<sup>-/-</sup> *Rag2*<sup>-/-</sup> mice.

To determine whether pathogenic microflora may be involved we tested the SPF1 and SPF2 colonies for *Helicobacter* species. *H. hepaticus* was identified as the only *Helicobacter* species in the SPF1 colony where colitis and colon cancer had been reestablished in *Tgfb1*<sup>-/-</sup> *Rag2*<sup>-/-</sup> mice. In the *Helicobacter*-free SPF2 colony, no colitis, hyperplasia, adenoma, or adenocarcinoma reappeared. These results suggest that *H. hepaticus* may be a causative factor for colitis in the *Rag2*<sup>-/-</sup> colonies, and that in the absence of TGF-1 the resulting hyperplasia can progress to adenoma and adenocarcinoma. This is consistent with the observation that *Smad3* knockout mice develop colon cancer when on a 129 genetic background (100% incidence) or a mixed 129 C57BL/6 background (30% incidence; Ref. 13). However, it is not known whether the colon cancer in these mice is associated with *H. hepaticus*. Another 129-strain *Smad3*<sup>-/-</sup> colony has been maintained free of *H. hepaticus*, and no colitis or adenocarcinoma has been observed.<sup>4</sup> In another study, immunodeficient C57BL/6J *Rag1*<sup>-/-</sup> mice were infected with *H. hepaticus* and *bilis* (14). In approximately one-third of the *Rag1*<sup>-/-</sup> mice inflam-

matory lesions with occasional hyperplasia were found, but no progression to adenoma or carcinoma was reported. None of the *Rag1*<sup>-/-</sup> mice had lesions. This study is consistent with our findings that adenoma/carcinoma but not inflammation/hyperplasia are dependent on genetic background, that *H. hepaticus* could be causative, and that colitis is not sufficient for progression to adenoma/carcinoma in this mouse model.

**DSS-induced Inflammatory Stress in TGF-1-deficient Mice.** Our experiments strongly suggest that inflammatory stress, while required, is not sufficient for the development of colon cancer in TGF-1-deficient mice. To test this hypothesis, *Tgfb1*<sup>-/-</sup> *Prkdc*<sup>scid/scid</sup> mice, which normally have inflammatory/hyperplastic lesions but which do not progress to colon cancer, were subjected to a significant increase in large intestinal inflammatory stress. DSS treatments (1.25% DSS, 60 days) were used to determine whether increased inflammatory stress might be sufficient to induce a transition from hyperplasia to adenoma/carcinoma in 6-8-week-old *Tgfb1*<sup>-/-</sup> *Prkdc*<sup>scid/scid</sup> mice. Subsets of animals were analyzed for cecum and colon lesions at 22, 29, and 32 days of treatment and at 2, 22, and 33 days after treatment. No adenomas or adenocarcinomas developed in DSS-treated mice (Fig. 4), suggesting that increasing inflammatory stress in the large intestine does not induce progression to adenoma and adenocarcinoma. As expected, both *Tgfb1*<sup>-/-</sup> and *Prkdc*<sup>scid/scid</sup> mice develop inflammation and moderate mucosal hyperplasia during treatment. However, the *Tgfb1*<sup>-/-</sup> *Prkdc*<sup>scid/scid</sup> mice are able to rapidly repair the mucosal damage, whereas inflammation and mucosal hyperplasia are still present in *Tgfb1*<sup>-/-</sup> *Prkdc*<sup>scid/scid</sup> mice 22 and 33 days after treatment. This supports previous evidence (6) suggesting that TGF-1-deficient mice may be less able to repair and maintain tissue damage than wild-type mice. These results confirm that inflammatory lesions are required for the development of colon cancer in TGF-1-deficient mice. However, because TGF-1-deficient mice on a *Prkdc*<sup>scid/scid</sup> (predominantly C3H) background all develop inflammatory lesions but rarely colon cancer, it is clear that inflammatory lesions are not sufficient for progression from hyperplasia to adenoma and adenocarcinoma.

**Comparison of Genetically Engineered Mouse Models of Colon Cancer.** Besides *Tgfb1 Rag2* double knockout mice, there are several other mouse models for human colon cancer: *Smad3*, *I12*, *I110*, *G*<sub>12</sub>, and *Muc2* knockout mice, and *Cdx2* and *Apc*<sup>Min</sup> heterozygous mice. SMAD3 is in the TGF-1 signaling pathway, and in its absence mice can develop metastatic colon cancer with associated inflammation (13). Similarly, *I110*, *Muc2*, and *G*<sub>12</sub> knockout mice, as well as *I12* and *2 microglobulin* (*2m*) double-knockout mice, all develop inflammatory bowel-associated colon cancer (Refs. 15, 16; reviewed in Ref. 17). *Cdx2* heterozygous mice develop primarily large intestinal and occasionally small intestinal tumors without loss of heterozygosity at the *Cdx2* locus, and there is no associated colitis, suggesting that mild disruption of normal topographical tissue relationships could alone initiate tumorigenesis (18). *Apc*<sup>Min</sup> mice have predominantly small intestinal adenomas with a few large intestinal tumors. Inhibition or elimination of inflammatory activity reduces the penetrance and multiplicity, but does not eliminate the tumor phenotype, so there may be a mild association of inflammation with the tumors, but it is not required (19). In most of the models in which a gene was knocked out that had no previous association with colon cancer, no evidence for other mutations in any genes normally associated with colon cancer were found. Similarly, in the *Tgfb1*<sup>-/-</sup>, *Smad3*<sup>-/-</sup>, and *Apc*<sup>Min</sup> models, no mutations were found in colon cancer genes other than the gene of the original mutation. An exception is the *I12 2m* double-knockout mouse in which mutations in *Apc* and *p53* were found (16). In summary, colitis seems to be required for tumorigenesis in most large intestinal cancer models in which *Apc* is not mutated. *Cdx2*

<sup>4</sup>J. Letterio, personal communication.

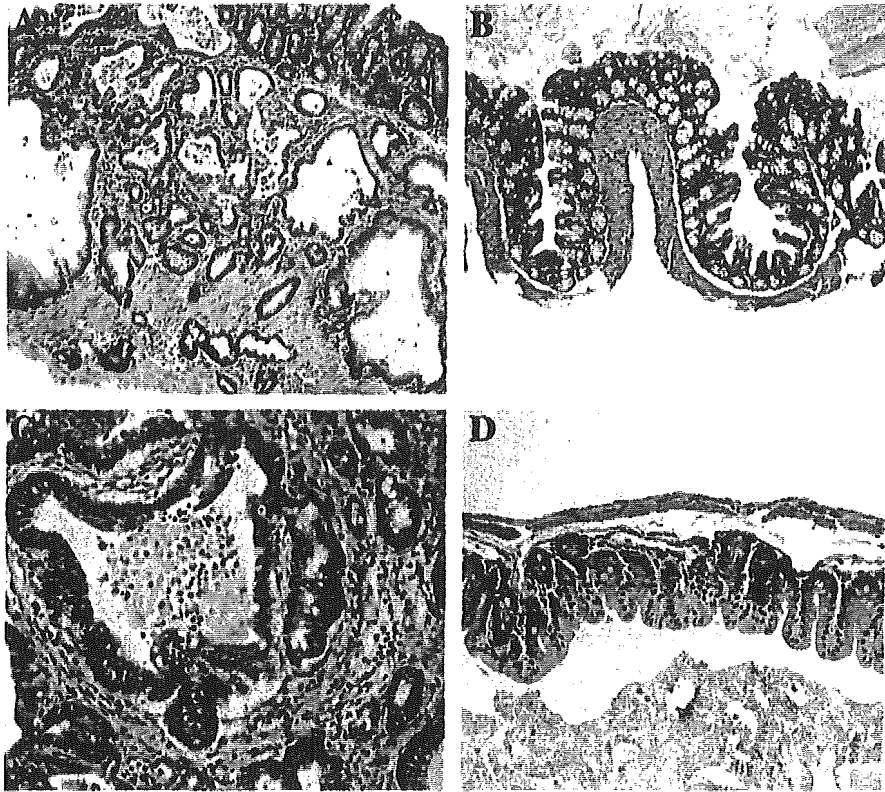


Fig. 3. Reconstitution of natural gut flora in germ-free *Tgfb1*<sup>-/-</sup> *Rag2*<sup>-/-</sup> mice. Representative samples are from previously germ-free *Tgfb1*<sup>-/-</sup> *Rag2*<sup>-/-</sup> mice that were reintroduced into barrier rooms SPF1 in which *H. hepaticus* was present (A and C) or SPF2 in which *H. hepaticus* was not present (B and D). A, adenocarcinoma from cecum of a 3-month-old mouse ( 25 magnification). B, no significant lesions from colon of a 4-month-old mouse ( 25 magnification). C, adenocarcinoma from cecum of a 4-month-old mouse ( 50 magnification). D, no significant lesions from cecum of a 6-month-old mouse ( 20 magnification).

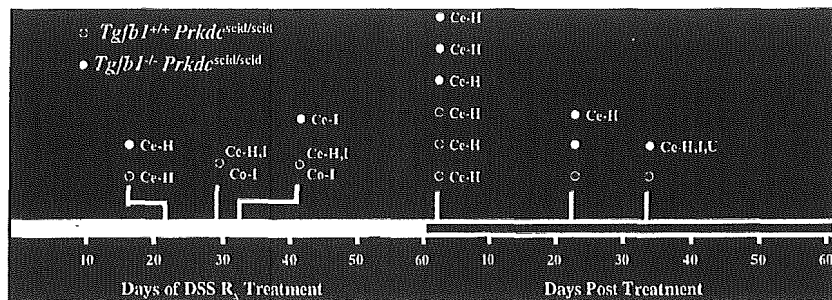
heterozygous mice are an exception because they develop grossly altered crypt architecture without colitis, and *Apc*<sup>fl/min</sup> mice are an exception because they can be made germ-free without major loss of the tumor phenotype (19). Progression to tumors could result either directly from deficiency in a tissue architecture gene, as in the *Cdx2* heterozygous mice, or through an inability of the epithelium to maintain tissue integrity in the presence of inflammatory stress. Altered inflammatory response and a deficiency in maintenance of tissue architecture may combine to induce large intestinal cancer in *Smad3*, *Tgfb1 Rag2*, *Il10*, and *G12* knockout mice.

**Interplay between Microbial Flora and Host Response Establishes Conditions for Colon Cancer.** Together, these results demonstrate that neither enteric microbial agents nor inflammation alone cause colon cancer in *Tgfb1*<sup>-/-</sup> *Rag2*<sup>-/-</sup> mice. Because genetic background also plays an important role in the process, it is clear that the response to the microbial-induced inflammation is critical to the development of colon cancer. This is consistent with evidence that a single microbial agent can have important modulatory effects on the host expression profile, especially in areas of nutrient absorption,

mucosal barrier fortification, xenobiotic metabolism, and angiogenesis (20). Consequently, to fully understand the conditions that lead to colitis-associated colon cancer in mice, the causative microbial agent(s), and the differential responses of the host inflammatory system and colon epithelium will need to be systematically investigated. The existence of *Tgfb1*<sup>-/-</sup> *Rag2*<sup>-/-</sup> and *Tgfb1*<sup>-/-</sup> *Rag2*<sup>-/-</sup> mice, which have different susceptibilities to colitis-associated colon cancer, will be critical to these investigations.

**Relevance of *Tgfb1*<sup>-/-</sup> *Rag2*<sup>-/-</sup> Mice to Human Colon Cancer.** Having established that colitis can cause colon cancer in mice with mutations in the TGF- signaling pathway and that the causative factors involve an interplay between host tissue and inflammatory responses to specific component(s) of microbial flora, it is worthwhile to compare this mouse model with UC-associated colon cancer in humans. The original studies on mutations in the human *TGFBR2* gene found mutations in 90% of the 15–20% of all human tumors displaying MSI, and the loss was found to occur at a late stage of tumorigenesis (5). More recent studies have indicated that as much as 70% of microsatellite-stable colon cancer can also exhibit a blockade

Fig. 4. DSS treatment of *Tgfb1*<sup>-/-</sup> and *Prkdc*<sup>scid/scid</sup> mice. Mice were treated for 60 days with DSS, and examined for type of lesion at various days during treatment and after treatment. O, *Tgfb1*<sup>-/-</sup> *Prkdc*<sup>scid/scid</sup> mice; O, without type of lesion given indicates normal cecum and colon in *Tgfb1*<sup>-/-</sup> *Prkdc*<sup>scid/scid</sup> mice; ●, *Tgfb1*<sup>-/-</sup> *Prkdc*<sup>scid/scid</sup> mice; Ce, cecum; Co, colon; H, hyperplasia; I, inflammation; U, ulceration.



of TGF- signaling (21), and in these cases the stage at which the tumor-suppressive activity of TGF- occurs is not clear. In one study of colon cancer in patients with UC, chromosomal instability preceded dysplasia (22). Consequently, it now seems plausible that human patients with UC can develop a genetic instability-induced disruption in TGF- signaling before or during early stages of tumor formation. This would be consistent with our studies on TGF-1-deficient mice.

It is not unreasonable to suggest that in humans years of inflammatory stress could eventually lead to mutations resulting in MSI and mutations in *TGFBR2* or downstream signaling genes. With a blockade in TGF- signaling the inflammatory stress could result in an altered inflammatory response and/or a disruption in tissue architecture, leading to an accelerated progression from hyperplasia to adenoma and adenocarcinoma. In *Tgfb1*<sup>-/-</sup> *Rag2*<sup>-/-</sup> mice the short 1–5-month period of inflammatory stress may be insufficient to generate genetic instability and subsequent mutations in *TGFBR2* or downstream signaling genes, but that would not be necessary because they already have a TGF- signaling defect.

#### Acknowledgments

We thank Wen Yun Sun for genotyping the mutant animals and Yong-Jin Kim for assistance with the manuscript.

#### References

- Kim, S. J., Im, Y. H., Markowitz, S. D., and Bang, Y. J. Molecular mechanisms of inactivation of TGF- receptors during carcinogenesis. *Cytokine Growth Factor Rev.*, *11*: 159–168, 2000.
- Manning, A. M., Williams, A. C., Game, S. M., and Paraskeva, C. Differential sensitivity of human colonic adenoma and carcinoma cells to transforming growth factor (TGF-): conversion of an adenoma cell line to a tumorigenic phenotype is accompanied by a reduced response to the inhibitory effects of TGF-. *Oncogene*, *6*: 1471–1476, 1991.
- Parsons, R., Myeroff, L. L., Liu, B., Willson, J. K., Markowitz, S. D., Kinzler, K. W., and Vogelstein, B. Microsatellite instability and mutations of the transforming growth factor type II receptor gene in colorectal cancer. *Cancer Res.*, *55*: 5548–5550, 1995.
- Jass, J. R., Do, K. A., Simms, L. A., Iino, H., Wynter, C., Pillay, S. P., Searle, J., Radford-Smith, G., Young, J., and Leggett, B. Morphology of sporadic colorectal cancer with DNA replication errors. *Gut*, *42*: 673–679, 1998.
- Markowitz, S., Wang, J., Myeroff, L., Parsons, R., Sun, L., Lutterbaugh, J., Fan, R. S., Zborowska, E., Kinzler, K. W., Vogelstein, B., Brattain, M., and Willson, J. K. V. Inactivation of the type II TGF- receptor in colon cancer cells with microsatellite instability. *Science (Wash. DC)*, *268*: 1336–1338, 1995.
- Engle, S. J., Hoying, J. B., Boivin, G. P., Ormsby, I., Gartside, P. S., and Doetschman, T. Transforming growth factor 1 suppresses nonmetastatic colon cancer at an early stage of tumorigenesis. *Cancer Res.*, *59*: 3379–3386, 1999.
- Boivin, G. P., Ormsby, I., Jones-Carson, J., O'Toole, B. A., and Doetschman, T. Germ-free and barrier-raised TGF-1-deficient mice have similar inflammatory lesions. *Transgenic Res.*, *6*: 197–202, 1997.
- Balish, E., and Filutowicz, H. Serum antibody response of gnotobiotic athymic and euthymic mice following alimentary tract colonization and infection with *Candida albicans*. *Can. J. Microbiol.*, *37*: 204–210, 1991.
- Kennedy, B. P., Payette, P., Mudgett, J., Vadas, P., Pruzanski, W., Kwan, M., Tang, C., Rancourt, D. E., and Cromlish, W. A. A natural disruption of the secretory group II phospholipase A2 gene in inbred mouse strains. *J. Biol. Chem.*, *270*: 22378–22385, 1995.
- Dieleman, L. A., Ridwan, B. U., Tennyson, G. S., Beagley, K. W., Bucy, R. P., and Elson, C. O. Dextran sulfate sodium-induced colitis occurs in severe combined immunodeficient mice. *Gastroenterology*, *107*: 1643–1652, 1994.
- Shull, M. M., Ormsby, I., Kier, A. B., Pawlowski, S., Diebold, R. J., Yin, M., Allen, R., Sidman, C., Proetzel, G., Calvin, D., and Doetschman, T. Targeted disruption of the mouse transforming growth factor-1 gene results in multifocal inflammatory disease. *Nature (Lond.)*, *359*: 693–699, 1992.
- Diebold, R. J., Eis, M. J., Yin, M., Ormsby, I., Boivin, G. P., Darrow, B. J., Saffitz, J. E., and Doetschman, T. Early-onset multifocal inflammation in the transforming growth factor-1-null mouse is lymphocyte mediated. *Proc. Natl. Acad. Sci. USA*, *92*: 12215–12219, 1995.
- Zhu, Y., Richardson, J. A., Parada, L. F., and Graff, J. M. Smad3 mutant mice develop metastatic colorectal cancer. *Cell*, *94*: 703–714, 1998.
- Burich, A., Hershberg, R., Waggle, K., Zeng, W., Brabb, T., Westrich, G., Viney, J. L., and Maggio-Price, L. Helicobacter-induced inflammatory bowel disease in IL-10- and T cell-deficient mice. *Am. J. Physiol.*, *281*: G764–G778, 2001.
- Velcich, A., Yang, W., Heyer, J., Fragale, A., Nicholas, C., Viani, S., Kucherlapati, R., Lipkin, M., Yang, K., and Augenlicht, L. Colorectal cancer in mice genetically deficient in the mucin *Muc2*. *Science (Wash. DC)*, *295*: 1726–1729, 2002.
- Sohn, K. J., Shah, S. A., Reid, S., Choi, M., Carrier, J., Comiskey, M., Terhorst, C., and Kim, Y. I. Molecular genetics of ulcerative colitis-associated colon cancer in the interleukin 2- and (2)-microglobulin-deficient mouse. *Cancer Res.*, *61*: 6912–6917, 2001.
- Fedorak, R. N., and Madsen, K. L. Naturally occurring and experimental models of inflammatory bowel disease. In: J. B. Kirsner and R. G. Shorter (eds.), *Inflammatory Bowel Disease*, 5 Ed., pp. 113–143. Philadelphia: WB Saunders Company, 1999.
- Chawengsaksophak, K., James, R., Hammond, V. E., Kontgen, F., and Beck, F. Homeosis and intestinal tumours in *Cdx2* mutant mice. *Nature (Lond.)*, *386*: 84–87, 1997.
- Dove, W. F., Clipson, L., Gould, K. A., Luongo, C., Marshall, D. J., Moser, A. R., Newton, M. A., and Jacoby, R. F. Intestinal neoplasia in the *ApcMin* mouse: independence from the microbial and natural killer (beige locus) status. *Cancer Res.*, *57*: 812–814, 1997.
- Hooper, L. V., Wong, M. H., Thelin, A., Hansson, L., Falk, P. G., and Gordon, J. I. Molecular analysis of commensal host-microbial relationships in the intestine. *Science (Wash. DC)*, *291*: 881–884, 2001.
- Grady, W. M., Myeroff, L. L., Swinler, S. E., Rajput, A., Thiagalasingam, S., Lutterbaugh, J. D., Neumann, A., Brattain, M. G., Chang, J., Kim, S. J., Kinzler, K. W., Vogelstein, B., Willson, J. K., and Markowitz, S. Mutational inactivation of transforming growth factor receptor type II in microsatellite stable colon cancers. *Cancer Res.*, *59*: 320–324, 1999.
- Rabinovitch, P. S., Dziadon, S., Brentnall, T. A., Emond, M. J., Crispin, D. A., Haggitt, R. C., and Bronner, M. P. Pancolonic chromosomal instability precedes dysplasia and cancer in ulcerative colitis. *Cancer Res.*, *59*: 5148–5153, 1999.

## Susceptibility of p53 -deficient Mice to Induction of Mesothelioma by Crocidolite Asbestos Fibers

Sean M. Marsella, Brenda L. Liu, Charles A. Vaslet, and Agnes B. Kane

Department of Pathology and Laboratory Medicine, Brown University School of Medicine, Providence, Rhode Island

- [Introduction](#)
- [Methods](#)
- [Results and Discussion](#)

---

### Abstract

Exposure of mesothelial cells to asbestos fibers in vitro has been shown to induce DNA damage mediated by oxidants. An early cellular response to DNA damage is increased expression of the p53 protein. This protein induces transcription of genes that activate cell cycle checkpoints or induce apoptosis. A murine mesothelial cell line that spontaneously acquired a point mutation in the p53 gene shows increased sensitivity to DNA damage induced by crocidolite asbestos fibers. It is hypothesized that p53 -deficient mice will show increased sensitivity to the genotoxic effects of asbestos and accelerated development of malignant mesotheliomas. -- Environ Health Perspect 105(Suppl 5):1069-1072 (1997)

Key words : p53 tumor suppressor gene, asbestos, mesothelioma

---

This paper is based on a presentation at The Sixth International Meeting on the Toxicology of Natural and Man-Made Fibrous and Non-Fibrous Particles held 15-18 September 1996 in Lake Placid, New York. Manuscript received at EHP 27 March 1997; accepted 27 May 1997.

This research was supported by grants R01 ES05712 and R01 ES03721 from the National Institute of Environmental Health Sciences.

Address correspondence to Dr. A.B. Kane, Department of Pathology and Laboratory Medicine, Brown University School of Medicine, Providence, RI 02912. Telephone: (401) 863-1110. Fax: (401) 863-9008. E-mail: [agnes\\_kane@brown.edu](mailto:agnes_kane@brown.edu)

Abbreviations used: TdT, terminal deoxynucleotide transferase; UICC, Union Internationale Contre le Cancer.

---

## Introduction

Diffuse malignant mesothelioma is a lethal neoplasm arising from the pleura, peritoneum, or pericardium. Most cases of mesothelioma are associated with a history of occupational exposure to asbestos; cases occurring after household or neighborhood exposure have also been reported ( 1 ). Asbestos fibers are classified in two categories: serpentine or chrysotile asbestos and amphiboles. Chrysotile consists of curly, white fibers and accounts for 90 to 95% of asbestos used commercially. Amphiboles are long, straight fibers and include crocidolite, amosite, anthophyllite, and tremolite. Although tremolite is not used commercially, this amphibole is a common contaminant of some deposits of sand, talc, and chrysotile asbestos. Malignant mesothelioma has also been associated with environmental exposure to tremolite asbestos or to erionite ( 2 ).

The mechanisms leading to the development of malignant mesothelioma are unknown. It is hypothesized that fiber geometry and dimensions, chemical composition, surface reactivity, and biopersistence in the lungs are important parameters related to toxicity ( 3 ). Asbestos fibers generate reactive oxygen species in a variety of cell-free assays [reviewed by Moyer et al. ( 4 )]. Macrophages exposed to asbestos fibers in vitro release reactive oxygen ( 5 ) and nitrogen species ( 6 ). The availability of iron at the surface of fibers is a critical parameter in catalyzing the generation of these highly reactive oxygen and nitrogen radicals ( 7 ). Ferric and ferrous cations are major components of amphibole asbestos fibers; iron may also be present as surface impurities on serpentine asbestos or some man-made fibers. Asbestos and other mineral fibers such as erionite may release or acquire iron from the surrounding medium, depending on the presence of chelators or reducing agents ( 8 ).

Several investigators have obtained evidence that reactive oxygen and nitrogen species contribute to DNA damage induced by asbestos fibers using a variety of target cell populations in vitro . Exogenous catalase or superoxide dismutase prevented DNA damage induced by asbestos in rat pleural mesothelial cells ( 9 ) or a human-hamster hybrid cell line ( 10 ). Crocidolite asbestos fibers induced formation of micronuclei in murine peritoneal mesothelial cells ( 11 ); this damage was also prevented by exogenous scavenging enzymes. Both reactive nitrogen intermediates and iron contribute to DNA damage induced by asbestos fibers in a human lung carcinoma cell line ( 12 ).

DNA breaks induced by oxidants, ionizing radiation, and chemotherapeutic drugs trigger a sequence of responses that arrest cells in the G1 phase of the cell cycle or induce apoptosis ( 13 ). A key event leading to these responses is increased expression of the p53 protein, followed by expression of additional genes that mediate cell cycle arrest or apoptosis. Cells lacking functional p53 protein as a result of gene deletion, formation of complexes with viral proteins, or point mutation are defective in cell cycle arrest or apoptosis triggered by DNA-damaging agents ( 14 ). Cistulli et al. ( 11 ) have shown that a murine mesothelial cell line that spontaneously acquired a point mutation in the p53 gene has increased susceptibility to induction of micronuclei by exposure to ionizing radiation or crocidolite

asbestos fibers in vitro .

Several strains of transgenic mice have been developed that carry one or two copies of a disrupted p53 allele ( 15 ). These mice show increased susceptibility to induction of micronuclei and tumors by ionizing radiation ( 16 ). Preliminary studies indicate that p53 -deficient mice show increased micronuclei in proliferating mesothelial cells after ip injection of crocidolite asbestos fibers. Therefore, we hypothesize that p53 -deficient mice will show increased susceptibility to induction of mesotheliomas by asbestos fibers.

## Methods

### In Vivo Studies

Homozygous (-/-), heterozygous (+/-), and wild-type (+/+) mice derived from the 129/Sv strain ( 17 ) were purchased from Jackson Laboratories (Bar Harbor, ME). Groups of 10 to 30 mice 6 to 8 weeks of age were injected weekly with 200  $\mu$ g ( $5.8 \times 10^8$  fibers) of Union Internationale Contre le Cancer (UICC) crocidolite asbestos suspended in 1.0 ml saline for 30 weeks. Mice were sacrificed as they developed ascites or weight loss. All experiments were conducted according to the guidelines established by the National Institutes of Health Guide for the Care and Use of Laboratory Animals. Histologic sections of all abdominal and thoracic organs were examined for the presence of tumors using the criteria described by Davis et al. ( 18 ). Malignant mesotheliomas were confirmed by expression of cytokeratins as evaluated by immunohistochemistry ( 19 ).

### In Vitro Studies

Primary murine mesothelial cells were isolated from peritoneal lavage fluid or following trypsinization of the peritoneal cavity as described previously ( 11 ). Wild-type (+/+) and homozygous p53 -deficient (-/-) mesothelial cells were maintained for 4 to 16 passages in vitro . Growth curves were generated as described previously ( 11 ). Preparation of metaphase spreads was carried out as described previously ( 20 ).

Apoptosis was induced in wild-type and p53 -deficient murine mesothelial cells by exposure to crocidolite asbestos ( $7.5 \mu\text{g}/\text{cm}^2$ ) ( 21 ) or camptothecin ( $10 \mu\text{g}/\text{ml}$ ) for 24 hr. Two assays for induction of apoptosis were used. DNA breaks with exposed 3' -OH ends were labeled by incorporation of biotinylated dUTP catalyzed by TdT; dUTP incorporation was detected by avidin-peroxidase immunohistochemistry using a kit purchased from Oncor, Inc. (Gaithersburg, MD). This assay was confirmed by agarose gel electrophoresis of low molecular weight DNA isolated from control and treated mesothelial cells. After ethidium bromide staining, a characteristic DNA ladder at 180-bp intervals was seen in apoptotic cells ( 22 ).

## Results and Discussion

Induction of Mesotheliomas in p53 -deficient Mice After 22 weekly ip injections, 12.5% of

**Table 1.** Incidence of malignant mesotheliomas in p53-deficient mice

|   | p53 Genotype   |                     |                     |
|---|----------------|---------------------|---------------------|
|   | -/-            | +/-                 | +/+                 |
| Fraction of mice with tumors <sup>a</sup> | 1/8<br>(12.5%) | 13/17<br>(76%)      | 9/28<br>(32%)       |
| Latency, weeks                            | 10             | 44 ± 2 <sup>b</sup> | 67 ± 1 <sup>c</sup> |

<sup>a</sup>The incidences of tumors and the genotypes are not independent;  $p = 0.003$  using Fisher's exact test.

<sup>b</sup>Mean ± SEM. <sup>c</sup>The mean latency between heterozygous +/- and wild-type +/+ mice is statistically significant;  $p = 0.002$  using Fisher's PLSD test.

the homozygous p53 -deficient mice developed mesotheliomas. The remainder of this cohort died with thymic lymphomas or hemangiomas that develop spontaneously in p53 -/- mice ( 23 ). After a mean latency of 44 weeks, 76% of the heterozygous p53 -deficient mice developed mesotheliomas compared to 32% of wild-type mice (Table 1). No spontaneous development of mesotheliomas has been observed in these genetically engineered mouse strains ( 23 ).

#### Accelerated development of malignant

mesothelioma induced by asbestos fibers in p53 -deficient mice could be explained by three mechanisms. First, p53 -deficient mesothelial cells could have a selective growth advantage over wild-type cells ( 24 ). Second, p53 -deficient mesothelial cells could have increased genetic instability secondary to loss of G1 arrest and incomplete repair of DNA damage ( 17 ). Genetic instability would predispose p53 -deficient cell populations to acquisition of additional mutations or deletions in cell cycle regulatory genes or tumor suppressor genes. Finally, p53 -deficient mesothelial cells may be resistant to apoptosis ( 25 ). These mechanisms were explored in vitro .

#### Growth and Apoptosis of p53 -deficient and Wild-type Mesothelial Cells in Vitro

Growth of early passage p53 +/+ and -/- murine peritoneal mesothelial cells was compared in vitro . The doubling time of p53 +/+ cells was approximately 24 hr, compared to only 12 hr for p53 -/- cells (Figure 1). The p53 +/+ cells were nearly diploid with a mean chromosome number of  $41 \pm 7$ , while p53 -/- cells were nearly tetraploid with a mean chromosome number of  $72 \pm 6$  (Figure 2). This observation is consistent with loss of a spindle checkpoint in p53 -deficient cells ( 26 ).

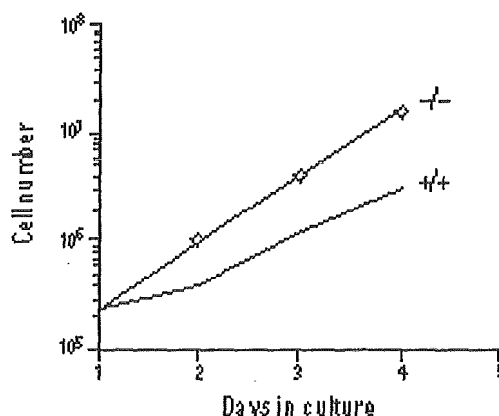


Figure 1 . Growth of wild-type p53 (+/+) and homozygous deficient p53 (-/-) mesothelial cell lines in vitro.

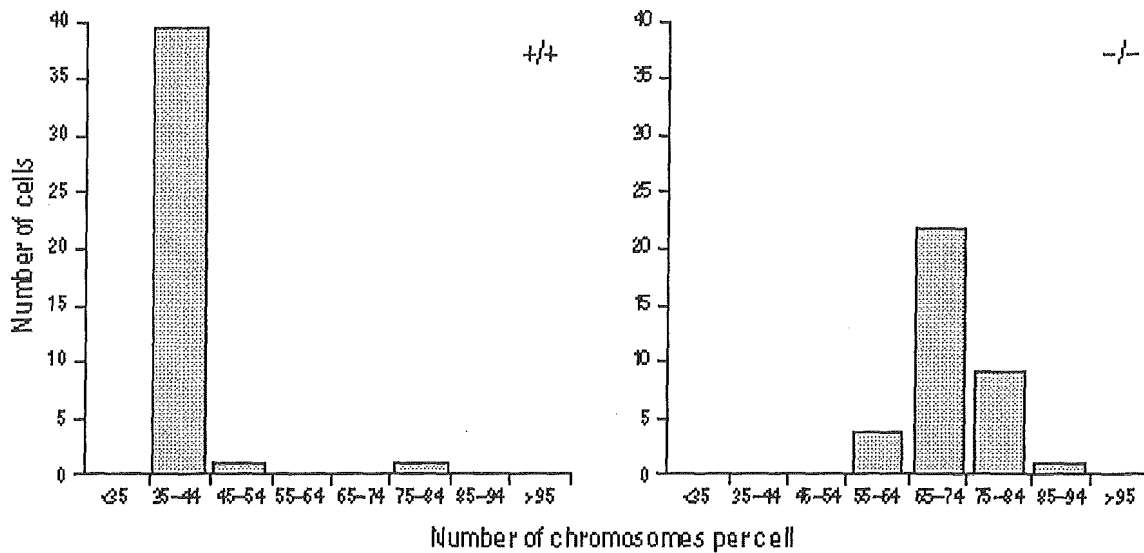


Figure 2 . Number of chromosomes determined on metaphase spreads of wild-type p53 (+/+) and homozygous deficient p53 (-/-) mesothelial cell lines in vitro after exposure to colcemid (0.2  $\mu\text{g}/\text{ml}$  for 1.5 hr).

**Table 2.** Induction of apoptosis by camptothecin in wild-type and p53-deficient murine mesothelial cells *in vitro*.

|              | p53 genotype    |                              |
|--------------|-----------------|------------------------------|
|              | -/-             | +/+                          |
| Control      | 0 $\pm$ 0       | 0.45 $\pm$ 0.23 <sup>a</sup> |
| Camptothecin | 0.13 $\pm$ 0.13 | 12.2 $\pm$ 2.7 <sup>b</sup>  |

<sup>a</sup>Percent of cells positive for apoptosis using 3'-OH end labeling; mean  $\pm$  SEM from three experiments.

<sup>b</sup>The difference between homozygous -/- and wild-type +/+ mesothelial cells is statistically significant;  $p = 0.002$  using Fisher's PLSD test.

Induction of apoptosis by ionizing radiation and chemotherapeutic drugs is p53 dependent (14). Early passage p53 +/+ mesothelial cells treated with crocidolite asbestos or camptothecin for 24 hr showed evidence of apoptosis as indicated by dUTP incorporation by TdT at 3'-OH ends of DNA (Table 2) and appearance of a DNA ladder on agarose gels (data not shown). In contrast, p53 -/- mesothelial cells were resistant to induction of apoptosis by exposure to crocidolite asbestos or camptothecin in vitro. Experiments are in progress to assess whether p53 -deficient

mesothelial cells show comparable resistance to apoptosis in vivo.

### Relevance of This Murine Model to Human Malignant Mesothelioma

Point mutations and deletions in the p53 tumor suppressor gene are relatively rare in human (27) and murine malignant mesothelioma cell lines (28). Patients with the Li-Fraumeni syndrome carry one mutated p53 allele and have an increased risk of developing sarcomas and brain, bone, breast, and adrenal cancers. A recent case-control study revealed a slightly increased risk of mesothelioma in people who were exposed to asbestos and had first degree relatives with the Li-Fraumeni syndrome (29). Despite infrequent point mutations in the p53 gene, human malignant mesotheliomas show overexpression of the p53 protein (30 - 32). A possible explanation for this paradoxical finding is a recent report that SV40-like DNA sequences and T-antigen have been identified in some human malignant mesotheliomas (33). Viral proteins such as SV40 T-antigen bind to the p53 protein, prolong its half-life, and inactivate its normal functions (14). Human malignant mesotheliomas are frequently aneuploid and show multiple cytogenetic abnormalities



34 ). This observation is consistent with increased genetic instability due to inactivation of p53 and abrogation of cell cycle checkpoints.

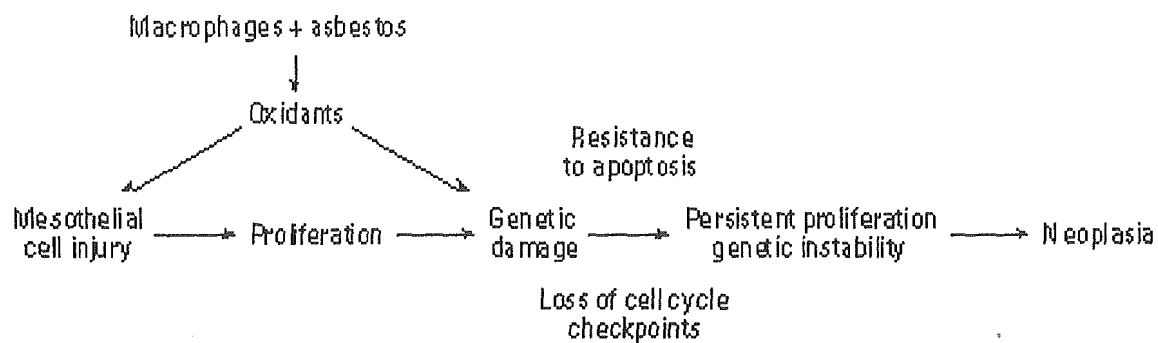


Figure 3 . Proposed mechanism for induction of malignant mesothelioma by asbestos fibers.

Figure 3 proposes the following hypothesis: The initial response of the mesothelial lining to asbestos fibers is injury that is repaired by proliferation ( 35 ). Production of oxidants by macrophages attempting to phagocytize asbestos fibers trapped at the mesothelial surface has been demonstrated in situ ( 36 ). It is hypothesized that macrophages release reactive oxygen and nitrogen species that induce DNA damage and apoptosis in mesothelial cells. Abrogation of p53 function by targeted deletion ( p53 -deficient mice) or inactivation by viral proteins (?humans) results in loss of cell cycle checkpoints and resistance to apoptosis in proliferating mesothelial cells. Functional inactivation of p53 or other components of the G1 cell cycle checkpoint ( 32 ) would accelerate later stages in the development and progression of malignant mesotheliomas induced by asbestos fibers.

## References

1. Churg AM, Green FHY. Occupational lung disease In: Pathology of the Lung. 2nd ed (Thurlbeck WM, Churg AM, eds). New York:Thieme Medical Publishers, 1995;851-930.
2. Bignon J. Mineral fibres in the non-occupational environment. In: Non-Occupational Exposure to Mineral Fibres. IARC Sci Publ No 90 (Bignon J, Peto J, Saracci R, eds). Lyon:International Agency for Research on Cancer, 1989;3-29.
3. McClellan RO, Miller FJ, Hesterberg TW, Warheit DB, Bunn WB, Kane AB, Lippmann M, Mast RW, McConnell EE, Reinhardt CF. Approaches to evaluating the toxicity and carcinogenicity of man-made fibers. Regul Toxicol Pharmacol 16:321-364 (1992).
4. Moyer VD, Cistulli CA, Vaslet CA, Kane AB. Oxygen radicals and asbestos carcinogenesis. Environ Health Perspect 102(Suppl 10):131-136 (1994).
5. Goodglick LA, Kane AB. Role of reactive oxygen metabolites in crocidolite asbestos toxicity to mouse macrophages. Cancer Res 46:5558-5566 (1986).
6. Thomas G, Ando T, Verma K, Kagan E. Asbestos fibers and interferon-  $\gamma$  up-regulate nitric oxide

- roduction in rat alveolar macrophages. *Am J Respir Cell Mol Biol* 11:707-715 (1994).
7. Fubini B. The possible role of surface chemistry in the toxicity of inhaled fibers. In: *Fiber Toxicology* (Warheit DB, ed). San Diego, CA:Academic Press, 1993;229-258.
  8. Hardy JA, Aust AE. Iron in asbestos chemistry and carcinogenicity. *Chem Rev* 95:97-118 (1995).
  9. Dong HY, Buard A, Renier A, Lévy F, Saint-Etienne L, Jaurand M-C. Role of oxygen derivatives in the cytotoxicity and DNA damage produced by asbestos on rat pleural mesothelial cells in vitro. *Carcinogenesis* 15:1251-1255 (1994).
  10. Hei TK, He ZY, Suzuki K. Effects of antioxidants on fiber mutagenesis. *Carcinogenesis* 16:1573-1578 (1995).
  11. Cistulli CA, Sorger T, Marsella JM, Vaslet CA, Kane AB. Spontaneous p53 mutation in murine mesothelial cells: increased sensitivity to DNA damage induced by asbestos and ionizing radiation. *Toxicol Appl Pharmacol* 141:264-271 (1996).
  12. Chao C-C, Park S-H, Aust AE. Participation of nitric oxide and iron in the oxidation of DNA in asbestos-treated human lung epithelial cells. *Arch Biochem Biophys* 326:152-157 (1996).
  13. Smith ML, Fornace AJ Jr. The two faces of tumor suppressor p53. *Am J Pathol* 148:1019-1022 (1996).
  14. Ko LJ, Prives C. p53 : puzzle and paradigm. *Genes Dev* 10:1054-1072 (1996).
  15. Sands A, Donehower LA, Bradley A. Gene-targeting and the p53 tumor-suppressor gene. *Mutat Res* 307:557-572 (1994).
  16. Lee JM, Abrahamson JLA, Kandel R, Donehower LA, Bernstein A. Susceptibility to radiation-carcinogenesis and accumulation of chromosomal breakage in p53 - deficient mice. *Oncogene* 9:3731-3736 (1994).
  17. Livingstone LR, White A, Sprouse J, Livanos E, Jacks T, Tlsty TD. Altered cell cycle arrest and gene amplification potential accompany loss of wild-type p53. *Cell* 70:923-935 (1992).
  18. Davis JM, Dungworth DL, Boorman GA. Concordance in diagnosis of mesotheliomas. *Toxicol Pathol* 24:662-663 (1996).
  19. Friedman MT, Gentile P, Tarectecan A, Fuchs A. Malignant mesothelioma. Immunohistochemistry and DNA ploidy analysis as methods to differentiate mesothelioma from benign reactive mesothelial cell proliferation and adenocarcinoma in pleural and peritoneal effusions. *Arch Pathol Lab Med* 120:959-966 (1996).
  20. Worton RG, Duff C. Karyotyping. In: *Methods in Enzymology*. Vol 58 (Jakoby WB, Pastan IH, eds). San Diego, CA:Academic Press, 1979;322-344.

21. Bérubé KA, Quinlan TR, Fung H, Magae J, Vacek P, Taatjes DJ, Mossman BT. Apoptosis is observed in mesothelial cells after exposure to crocidolite asbestos. *Am J Respir Cell Mol Biol* 5:141-147 (1996).
22. Richburg JH, Boekelheide K. Mono-(2-ethylhexyl) phthalate rapidly alters both Sertoli cell vimentin filaments and germ cell apoptosis in young rat testes. *Toxicol Appl Pharmacol* 137:42-50 (1996).
23. Donehower LA, Harvey M, Vogel H, McArthur MJ, Montgomery CA Jr, Park SH, Thompson T, Ford RJ, Bradley A. Effects of genetic background on tumorigenesis in p53 deficient mice. *Mol Carcinog* 14:16-22 (1995).
24. Harvey M, Sands AT, Weiss RS, Hegi ME, Wiseman RW, Pantazis P, Giovanella BC, Tainsky MA, Bradley A, Donehower LA. In vitro growth characteristics of embryo fibroblasts isolated from p53 - deficient mice. *Oncogene* 8:2457-2467 (1993).
25. Symonds H, Krall L, Remington L, Saenz-Robles M, Lowe S, Jacks T, Van Dyke T. p53 - dependent apoptosis suppresses tumor growth and progression in vivo . *Cell* 78:703-711 (1994).
26. Cross SM, Sanchez CA, Morgan CA, Schimke MK, Ramel S, Idzerda RL, Raskind WH, Reid BJ . A p53 -dependent mouse spindle checkpoint. *Science* 267:1353-1356 (1995).
27. Metcalf RA, Welsh JA, Bennett WP, Seddon MB, Lehman TA, Pelin K, Linnainmaa K, Pammilehto L, Mattson K, Gerwin BI, Harris CC. p53 and Kirsten- ras mutations in human mesothelioma cell lines. *Cancer Res* 52:2610-2615 (1992).
28. Cora EM, Kane AB. Alterations in a tumor suppressor gene, p53 , in mouse mesotheliomas induced by crocidolite asbestos. *Eur Respir Rev* 3:148-150 (1993).
29. Heineman EF, Bernstein L, Stark AD, Spirtas R. Mesothelioma, asbestos, and reported history of cancer in first-degree relatives. *Cancer* 77:549-554 (1996).
30. Kafiri G, Thomas DM, Shepherd NA, Krausz T, Lane DP, Hall PA. p53 expression is common in malignant mesothelioma. *Histopathology* 21:331-334 (1992).
31. Mayall FG, Goddard H, Gibbs AR. The frequency of p53 immunostaining in asbestos-associated mesotheliomas and non-asbestos-associated mesotheliomas. *Histopathology* 22:383-386 (1993).
32. Segers K, Backhovens H, Singh SK, De Voecht, J, Ramael M, Van Broeckhoven C, Van Marck E. Immunoreactivity for p53 and mdm2 and the detection of p53 mutations in human malignant mesothelioma. *Virchows Arch* 427:431-436 (1995).
33. Carbone M, Pass HI, Rizzo P, Marinetti MR, Di Muzio M, Mew DJY, Levine AS, Procopio A. Simian virus 40-like DNA sequences in human pleural mesothelioma. *Oncogene* 9:1781-1790 (1994).
34. Taguchi T, Jhanwar SC, Siegfried JM, Keller SM, Testa JR. Recurrent deletions of specific

chromosomal sites in 1p, 3p, 6q, and 9p in human malignant mesothelioma. *Cancer Res* 53:4349-4355 (1993).

35. Moalli PA, Macdonald, JL, Goodglick LA, Kane AB. Acute injury and regeneration of the mesothelium in response to asbestos fibers. *Am J Pathol* 128:426-445 (1987).

36. Goodglick LA, Kane AB. Cytotoxicity of long and short crocidolite asbestos fibers in vitro and in vivo. *Cancer Res* 50:5153-5163 (1990).

---

[ [Table of Contents](#) ] [ [Citation in PubMed](#) ] [ [Related Articles](#) ]

Last Update: October 27, 1997